EFFECT OF MAGNETIC ANISOTROPY ON COERCIVITY OF PARTICLES FOR MAGNETIC RECORDING

Mikio Kishimoto

EFFECT OF MAGNETIC ANISOTROPY ON COERCIVITY OF PARTICLES FOR MAGNETIC RECORDING

Mikio Kishimoto

Hitachi Maxell Co. Ltd.

(November, 1979)

Abstract

To improve the recording density of a magnetic recording tape, it has been studied to increase the coercivity of magnetic materials used in the recording tape. The cobalt-substituted iron oxides have the advantage that the coercivity can be increased up to about 2000 Oe by the crystalline magnetic anisotropy of cobalt ions. However, the material has the disadvantage that the coercivity becomes unstable not only at high temperature but also during aging.

The origin of the instability of the cobalt-substituted iron oxides was studied focussing the attention on the role of Fe^{2+} in oxides, and the following behaviors were clarified. The instability of coercivity was caused by the variation of the magnetic anisotropy induced by the migration of Co^{2+} to the stable sites in spinel lattice due to the demagnetizing field of acicular particles. The migration of Co^{2+} was helped by Fe^{2+} ions and the instability of coercivity was actually more pronounced in the oxides containing more amount of Fe^{2+}.

To get rid of the instability of coercivity of the cobalt-substituted iron oxides, the epitaxial growth of iron-cobalt ferrite, of which composition is approximately of $CoFe_2O_4$, was tried and successfully assured on the surface of γ-Fe_2O_3 particles. The coercivity of the oxides was observed as extremely stable compared with that of cobalt-substituted iron oxides. The stability was accounted for by considering the difficulties of migration of Co^{2+} ions which were just on the surface of γ-Fe_2O_3 particles. Furthermore, the coercivity itself of the oxides remarkably

increased, and it was clarified caused by the magnetic anisotropy of the iron-cobalt ferrite on the γ-Fe_2O_3 particles.

Although MnBi particles have been studied as a permanent magnet material, there is only few report on the investigation to utilize the MnBi particles for magnetic recording material. In this study, the preparation method and the magnetic properties of MnBi particles were examined for the purpose of utilizing the particles for permanent recording material. The thin plate-shaped MnBi particles of which size is nearly 0.5 μm, and has the coercivity of 16000 Oe at room temperature were obtained by grinding MnBi block prepared by a sintered method, in a ball mill. The MnBi particles were dispersed in a polymer binder, and oriented by a magnetic field. The magnetic properties were examined for the oriented particles, and the following behaviors were clarified. The temperature dependence of the coercivity nearly agreed with the calculated result by assuming the particles of single-domain. The MnBi particles could be easily demagnetized by cooling down to liquid nitrogen temperature, although the particles were difficult to be demagnetized at room temperature due to the high coercivity. After the demagnetization by cooling, the MnBi particles could be easily magnetized at room temperature, and the coercivity increased with increasing the strength of an applied magnetic field. These results suggested that "nuclei" existed in the demagnetized particles and they disappeared by applying a strong magnetic field at room temperature. These properties showed the possibility of MnBi particles to be utilized for the permanent recording material.

Contents

1. Introduction

1.1. Particles for Magnetic Recording

1.1.1. Historical Outline

The earliest conventional recording tapes were those developed in Germany for the Magnetophon recorder before 1939. The particle used were roughly spherical and about 1 μm in diameter. When compared with the coercivity of today's acicular iron oxide particles having 260-500 Oe, the coercivity of the early particles was so low as 90 Oe or at most 150 Oe. Naturally, the output signal obtained from tapes made of these particles was low. In 1954, Camras discovered that the coercivity of tape would remarkably be increased by using acicular-shaped particles.[1] Since this discovery, the acicular-shaped γ-Fe_2O_3 particles have been used for the most popular material in magnetic recording tape.[2] Thereafter, the investigations of γ-Fe_2O_3 or other crystal particles have all been in a direction to increase the particle coercivity itself up to the highest value.[3,4]

Although the ferromagnetic properties of CrO_2 were known from earlier date,[5] it was only recently in 1955 that the crystal was investigated to utilize as the material having a great recording potential.[6] From 1958, a technique was culminated till the crystal was finally used in the short wave-length region with a high signal to noise ratio.[7] The morphology of CrO_2 had a high degree of perfection as a result of high dispersibility in some binder substances.

Another approach to increase the coercivity was to introduce

magnetic anisotropy by substituting Co^{2+} ions in the γ-Fe_2O_3. The idea, in fact, has been examined since more than 20 years. It was found that the approach resulted the thermal and aging effect in the material. There was only a few of temporary success in commercial base.[8] However, to compete with CrO_2, the cobalt-substituted iron oxides have been investigated in recent years. Actually, the American 3 M company introduces the so-called High-Energy tape. In Japan, a similar tape is fabricated by T.D.K. These tapes have a coercivity compatible with the CrO_2 tapes. Their signal is indeed markedly higher than that of γ-Fe_2O_3 tapes.[9] However, the instability of coercivity has still been left as a subject to be overcome.

In 1972, Hitachi Maxell Co. Ltd. in Japan invented a method to crystallize iron-cobalt ferrite on the surface of γ-Fe_2O_3 instead of substituting cobalt ions in the entire region of the crystal of γ-Fe_2O_3. The coercivity showed extremely stable character in both high temperature and aging. Also, the coercivity could be controlled in the range about 400 to 1500 Oe by adjusting the quantity of cobalt ions.

The metallic iron and alloys of iron and cobalt have been expected to get the high output level due to the high saturation magnetization.[10] Yet no application was found in magnetic recording. The reasons were difficulties for the preparation of homogeneous particles with the desired morphology, chemical instability and its poor dispersibility in binder. Nevertheless, the research on these alloys has been continued getting the provisional success in near future.

1.1.2. Oxide Particles

γ-Fe_2O_3

The material has a cubic symmetry with a spinel lattice whose lattice parameter and density is 8.34 Å and 4.9 g/cm^3 respectively. It has crystalline magnetic anisotropy K_1=-4.64x10^3 erg/cm^3.[11] This small anisotropy means that the desired magnetic hardness must be given by the shape anisotropy. Consequently it has long been tried to make the particles with acicular shape. The available γ-Fe_2O_3 particles consist of needles whose long axis is in the direction of (110).[12] The preparation method of acicular shaped γ-Fe_2O_3 was initially proposed by Camras.[1] First acicular α-FeOOH is prepared, then reduced to Fe_3O_4, and finally converted to γ-Fe_2O_3 :

$$\alpha\text{-FeOOH} \xrightarrow[300\text{-}600^\circ C]{-} \alpha\text{-}Fe_2O_3 \xrightarrow[300\text{-}400^\circ C]{-} Fe_3O_4 \xrightarrow[250\text{-}300^\circ C]{-} \gamma\text{-}Fe_2O_3.$$

The morphology of the γ-Fe_2O_3 thus depends considerably on that of the starting α-FeOOH. During the convertion from α-FeOOH to γ-Fe_2O_3, the formation of agglomerates occurs. The formation of agglomerates is enhanced as the convertion temperature is higher. On the other hand, during the stage of the dehydration, holes and fissures are formed, which may partly disappear at higher temperature. It can be concluded that the preparation technique of γ-Fe_2O_3 comprises to a large extent of the controlling reaction parameters that govern the convertion of α-FeOOH into γ-Fe_2O_3. At present, the coercivity of γ-Fe_2O_3 can be controlled in the range of about 250 to 500 Oe.[3]

CrO_2

CrO_2 has a tetragonal crystal structure with a=4.41 Å and c=2.91 Å. The density is 4.9 g/cm^3. The CrO_2 used for recording purpose consists of elongated submicron particles in the direction of (001).[13] The crystal anisotropy is relatively large, $K=+2.5\times10^4$ erg/cm^3.[13] CrO_2 is prepared in a technical scale by the decomposition of CrO_3 under hydrothermal condition. For a good reaction kinetics and a good morphology of the end product, a control is required in the nucleation process of the particles. In the patent literature, numerous proposals appear as the appropriate dope. An excellent dope is Sb_2O_3. The coercivity can be controlled to exist in the range of about 400 to 1000 Oe.

Cobalt-substituted γ-Fe_2O_3

Another approach to increase the coercivity is to introduce crystal anisotropy by substituting Co^{2+} ions in the spinel lattice. This does not change the crystal structure. The anisotropy constant, however, changes from the negative value of γ-Fe_2O_3 to a positive value, the amount of the change depending on the quantity of Co^{2+} ions in the lattice. The easy axis shifts from (111) to (100) direction. The preparation of cobalt-substituted γ-Fe_2O_3 is carried out according to the patent reference by soaking iron oxides with a solution of Co^{2+} salt before the subsequent convertion to γ-Fe_2O_3,[14,15] or by carrying out the oxidation of Fe^{2+} to FeOOH in the presence of Co^{2+} ions,[16,17] or by heating in an autoclave the co-precipitant of cobalt and iron hydroxides from alkaline solution.[18] Although this

material has advantage to increase its coercivity up to about 2000 Oe, the built up coercivity, on the other hand, shows a grave weakness against high temperature under which the diffusion of cobalt ions takes place in the spinel lattice, destroying easily the magnetic characteristics.

1.1.3. Metal Particles

Fe-Co alloys

Iron has cubic bcc structure with a=2.866 Å at room temperature. The X-ray density is 7.86 g/cm^3. The crystalline anisotropy, being K_1=4.8x10^4 erg/cm^3, is too low to attain the required coercivity. Therefore, also for this material the main facter controlling the magnetic anisotropy must be due to the shape. Metal particles have been searched for material on the base of Fe. There exist following three in producing the elongated particles: 1) Reduction of a solution of Fe^{2+} salt in the aid of $NaBH_4$,[19] 2) Pseudomorphic reduction of iron oxides with H_2,[20] 3) Evaporation method of iron in an inert gas at low pressure.[21] Tapes prepared with these particles show a high output gain in a region of short wave-length twice as high as that of CrO_2 tape.[22] However, no data have been available on the noise of the tape and its chemical stability.

MnBi

MnBi is a ferromagnetic intermetallic compound with NiAs-structure.[23] This compound shows strong uniaxial anisotropy whose K is 11.6x10^6 erg/cm^3 along the c-axis at room temperature.

A satisfactory high pure MnBi can be prepared by the usual sintering method. The remarkable increase of coercivity in MnBi particles was reported to occur while its particle size is being reduced, the highest value reaching 12000 Oe for the 3 μm particles.[24] MnBi particles have been investigated on a permanent magnet material due to the high coercivity. On the other hand, the anisotropy energy of MnBi is reported to decrease rapidly with decreasing temperature and to pass through zero at 84 K.[25] This anomalous decrease in the anisotropy energy enables to write many signals into the tape at low temperature, being, therefore, called "low temperature recording". An actual application of this recording is hereby reported in due course.

1.2. Manufacturing of Magnetic Recording Tape

Several preliminary stages are required in the preparation of our magnetic recording tape till the final coating stage is to be completed. The basic requirements in each stage are described in the following.

Magnetic paint

Magnetic paint is prepared by dispersing magnetic particles in polymer binder soluble in soluvents such as toluene or methyl ethyl ketone. Stabilizer, plasticizer, and lubricants are usually used in the dispersion process. A ball mill is the most popular method of the particles dispersion. Steel balls act to unfasten the particles wide apart from each other to disperse them uniformly throughout the entire mixture to form magnetic paint.

Coating process

The above mentioned magnetic paint is coated on a base film with uniform thickness. There are many devices in the coating techniques successfully adopted such as these called reverse roll, gravure coating, or knife-brade coating respectively. Polyethylene terephthalate is considered to be the most popular material to be used for our base film.

Alignment of particles

During and after the coating process while the surface of the tape is still so viscous that the magnetic particles in the paint may move freely around the tape, a magnetic field is superimposed. When the tape is completely dried, preferred orientation of the magnetic particles is easily available in the direction of the magnetic field.

Tape surface smoothing

Since each particle is in the form of long needle, some of them are bounded to project from the tape surface. These projected particles must be smoothed out. To achieve this the binder is first softened by heating and then the projected particles are embedded into the tape by using a special roller whose surface is so refined as a mirror.

Slitting

The wide webs of smoothing magnetic tape must be parted away so that suitable widths to fit the various tape recorders may be made, for exsample, 1/4 inch wide audio cassette tape, or 1/2 inch audio open tape. In the process a high-speed precision slitting machine is usually used.

1.3. Purpose of This Study

Since the magnetic recording technique was developed, a continuous improvement has been evolved to increase the recording density in the tape. The recording density usually increases with increasing the coercivity of a tape. Much has been studied on a problem as to how we can increase the particle coercivity. At present, acicular γ-Fe_2O_3 particles with diameter of about 0.5 μm are widely used for the magnetic recording material. The present technical limitting value in the coercivity is 500 Oe in the case of γ-Fe_2O_3. This value of coercivity is satisfactory in the materials used so far in the ordinary audio tapes. However, further higher coercivity, 500–1000 Oe is required in the higher quality audio tapes or video tapes, which need the higher recording density. For the material in this field, cobalt-contained iron oxides are the main material in the present industry. The coercivity of the material can be increased up to about 2000 Oe by adjusting the cobalt content. For the material having the coercivity higher than 2000 Oe, MnBi particles are promising. MnBi particles have the possibility to be utilized for permanent recording material.

The investigation to increase the coercivity of magnetic recording material has been considerably advanced, and at present, the coercivity up to about 2000 Oe can be obtained in the industrial scale. However, many have been remained still unsolved on the efficient preparation of especially good recording material. Especially on the factors influencing the coercivity of the material, there appears a very little report.

In this thesis, the magnetic recording material is classified into three classes such as that of γ-Fe_2O_3 particles, that of cobalt-contained iron oxide particles, and that of MnBi particles according to the respective strengths of coercivities. The main magnetic anisotropy of the materials is shape anisotropy for γ-Fe_2O_3 particles, crystalline and induced anisotropy for cobalt-contained iron oxide particles, and crystalline anisotropy for MnBi particles. In order to make further progress of the magnetic recording material, the effect of the anisotropies on the coercivity is to be studied in detail.

2. Coercivity of γ-Fe_2O_3 Particles

2.1. Effect of Crystallite Size on Coercivity of γ-Fe_2O_3

Acicular γ-Fe_2O_3 particles are main pigments of magnetic recording tape. At present, commercially available γ-Fe_2O_3 particles are usually prepared in the following procedure. Acicular α-FeOOH are first dehydrated to α-Fe_2O_3, subsequently reduced to Fe_3O_4, and then oxidized to γ-Fe_2O_3. In this procedure, the magnetic properties of resulting γ-Fe_2O_3 particles are considerably influenced by the dehydration temperature. In this investigation, the influence of the dehydration temperature of α-FeOOH particles on the coercivity of γ-Fe_2O_3 particles was examined.[26)]

The electron micrograph of α-FeOOH used as a starting material is shown in Fig. 2.1(a). The α-FeOOH particles were dehydrated at each temperature of 300, 400, 500, 600, 700, and 800°C for 1 h, respectively, while fresh air was circulated. These six kinds of samples of α-Fe_2O_3 were reduced to Fe_3O_4 at 350°C for 30 min in hydrogen gas containing water vapour, and then converted to γ-Fe_2O_3 by oxidizing at 250°C for 30 min in air. The saturation magnetization of these γ-Fe_2O_3 samples was 74 emu/g at 300 K, being independent of the dehydration temperature. Fig. 2.1(b)-(g) show the electron micrographs of these samples of γ-Fe_2O_3 particles. Below 600°C, the acicular shape of the starting material is essentially retained. But at 700°C, neighbouring particles begin to sinter together, and above 800°C, the formation of agglomerated particles are observable.

The crystallite size of γ-Fe_2O_3 particles was determined from X-ray diffraction line broadening measurement using Scherrer

equation.[27,28] Fig. 2.2 shows the relation between the dehydration temperature and the average value of each crystallite size measured in (220), (313), (400), (333), and (440). In the samples dehydrated below 500°C, the average crystallite size is independent of temperature, and is about 410 Å. The growth of crystallite is observed in the samples dehydrated above 600°C. In the dehydration at 800°C, the crystallite size becomes about 500 Å.

The coercivity of dehydrated γ-Fe_2O_3 was measured on the particles only compressed to have the density of 1.1-1.3 g/cm^3 at 300 K and 85 K using a vibrating sample magnetometer.[29] Fig. 2.3 shows the relation between the coercivity at 300 K and 85 K and the dehydration temperature. In both 300 K and 85 K, the maximum coercivity is observed in the neighbourhood of 600°C. The abrupt decrease at 800°C is clearly caused by the agglomeration of particles. The ratio of coercivity at 85 K to that at 300 K is shown in Fig. 2.4. The ratio decreases as the dehydration temperature is increased. If the coercivity of acicular γ-Fe_2O_3 particles is proportional to $Hc=2\pi Is$, the ratio of coercivity is calculated to be 1.09 by using the saturation magnetization Is of 81 emu/g measured at 85 K. The measured ratio of coercivity is larger than 1.09 in any samples. Fig. 2.5 shows the magnetization curve at 300 K of these samples of γ-Fe_2O_3 particles. The value of magnetization in Fig. 2.5 is normalized by the value of each sample under 10 kOe. It is noted that the sample dehydrated at higher temperature is easy to be magnetized. These results can be explained by considering that crystallites showing superparamagnetic behavior exist in the

the particles. When dehydration temperature is increased, the growth of crystallite is enhanced, and superparamagnetic crystallites are considered to decrease.

Berkowitz found the superparamagnetic behavior on crystallite whose diameter is below 300 Å. He considered that a stable single-domain is lying in a range around approximately 400 Å at room temperature.[30] In this investigation, the average crystallite size of sample having the maximum coercivity is about 420 Å. This value is close to that of the critical crystallite size of single-domain behavior reported by Berkowitz. The average crystallite size of the sample dehydrated at 800°C is about 500 Å, and superparamagnetic behavior is observed even in this sample. This indicated that the distribution of crystalline size in the particles is considerably broad.

(a) Starting α-FeOOH

0.5 μm

Fig. 2.1 Electron micrographs of α-FeOOH and γ-Fe_2O_3 particles. (a) is α-FeOOH particles of starting material. (b)-(g) are γ-Fe_2O_3 particles prepared from α-FeOOH particles by dehydrating at various temperatures.

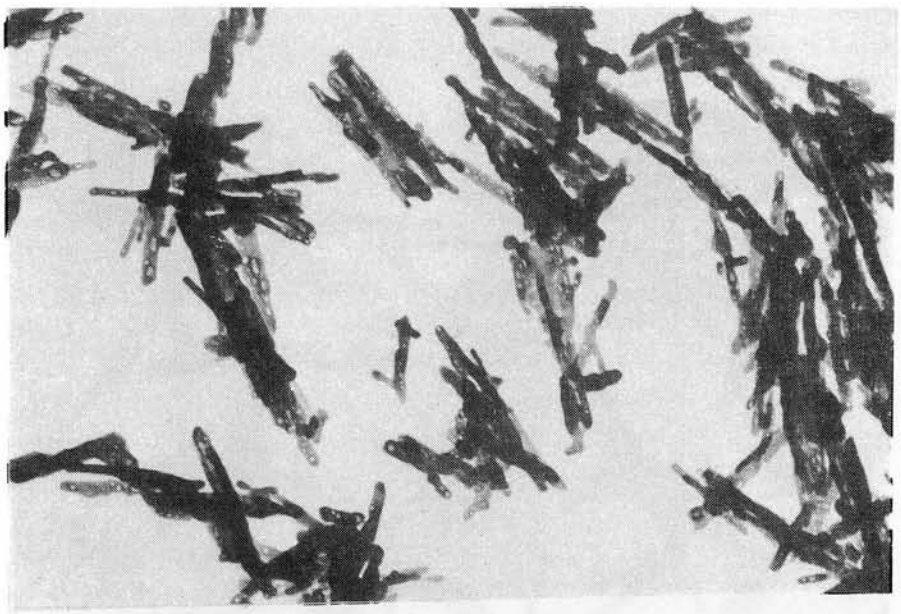

(b) 300°C

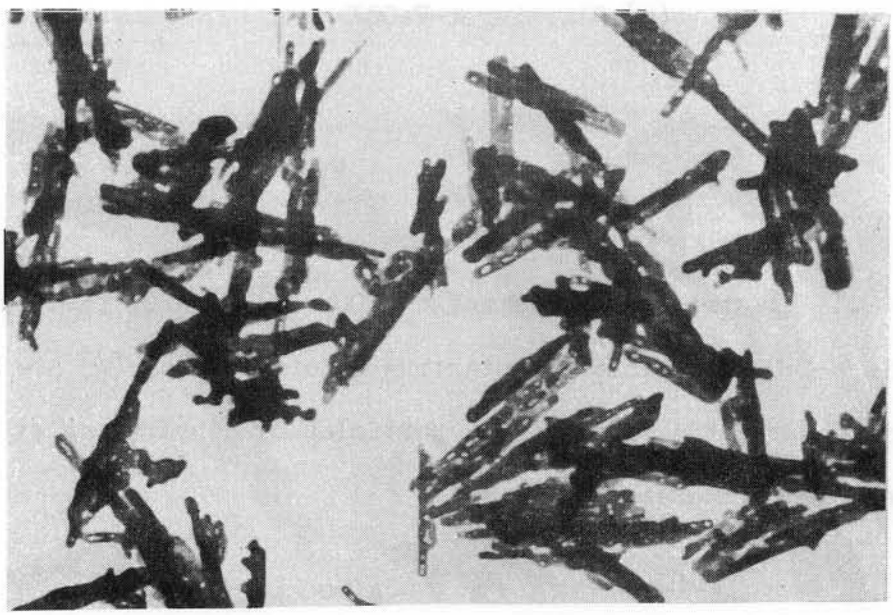

(c) 400°C

0.5 μm

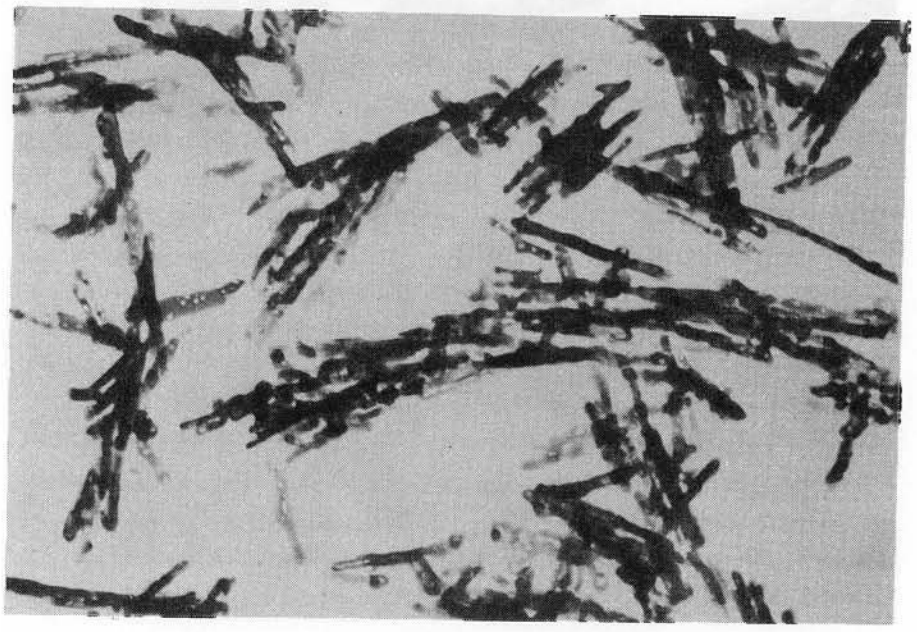

(d) 500°C

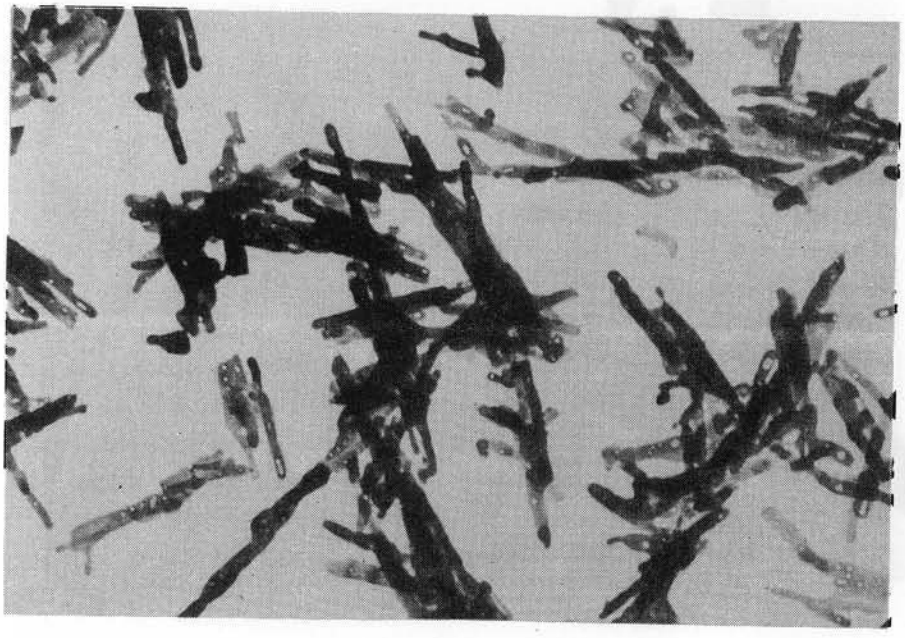

(e) 600°C

0.5 μm

(f) 700°C

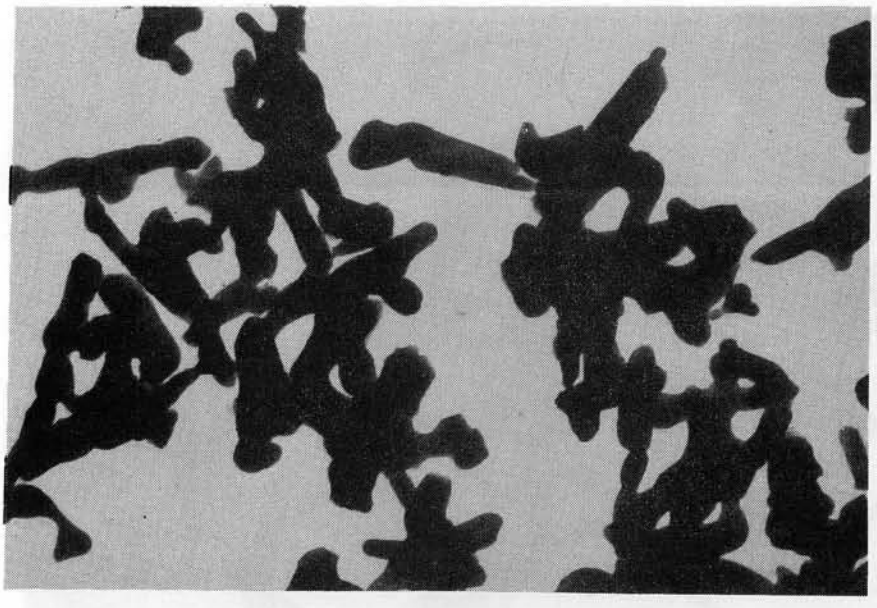

(g) 800°C

0.5 μm

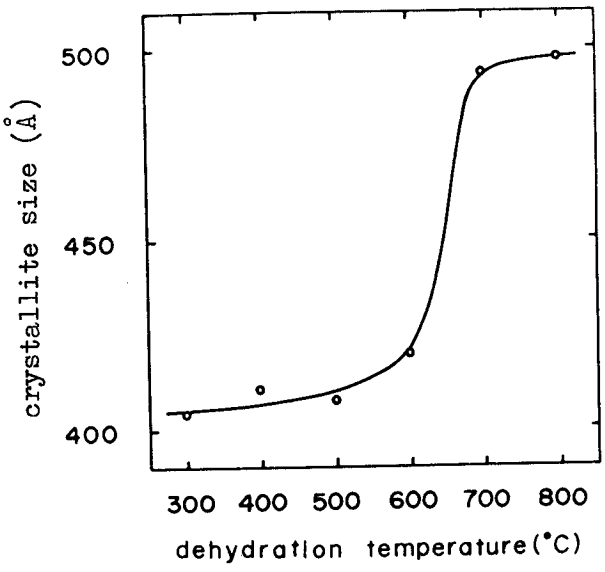

Fig. 2.2 Relation between average crystallite size of γ-Fe_2O_3 particles and dehydration temperature.

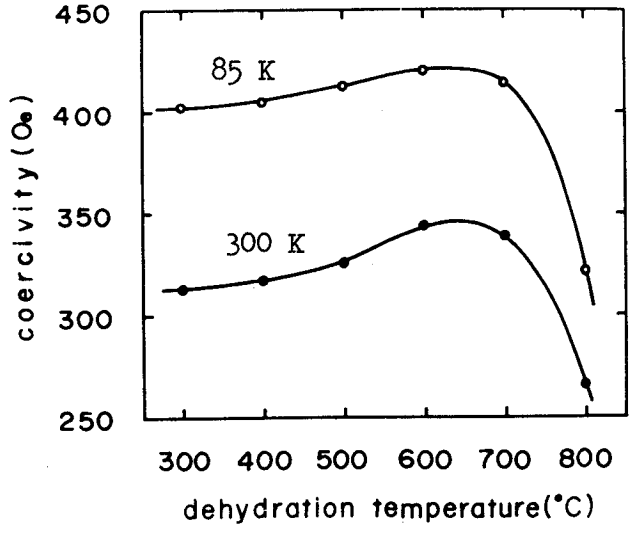

Fig. 2.3 Relation between coercivity at 300 K and 85 K of γ-Fe_2O_3 particles and dehydration temperature.

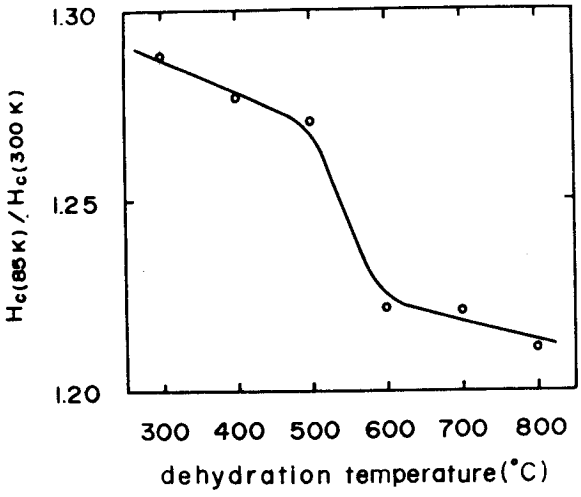

Fig. 2.4 Relation between the ratio of coercivity Hc(85K)/Hc(300K) and the dehydration temperature.

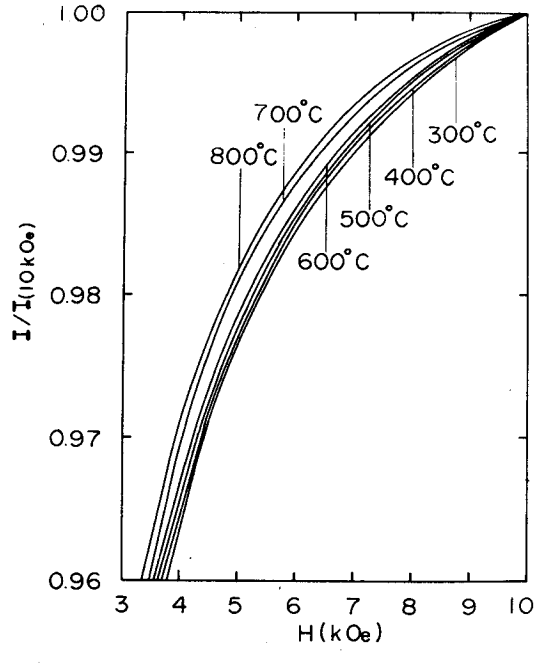

Fig. 2.5 Magnetization curve at 300 K of γ-Fe_2O_3 particles with various temperatures.

2.2. Angular Dependence of Coercivity of Oriented γ-Fe_2O_3 Particles

In the previous section 2.1., the highest coercivity of γ-Fe_2O_3 particles obtained is 350 Oe at room temperature. The value of coercivity is considerably lower than the value 2600 Oe which is calculated from the shape anisotropy $2\pi I_s$. To clarify the origin of the low coercivity, the angular dependence of coercivity of oriented γ-Fe_2O_3 particles was measured.

The γ-Fe_2O_3 particles shown in Fig. 2.1(e) were dispersed well in a polymer binder with the packing density of about 50 volume percent and oriented under the magnetic field of 1500 Oe. The dependence of the coercivity of the oriented γ-Fe_2O_3 particles on the angle θ between the direction of orientation and the direction of measurement was measured. The result is shown in Fig. 2.6. The coercivity slightly increases with increasing the angle θ, and in the neighbourhood of 60°, the coercivity shows the maximum value of 380 Oe.

When the magnetization reversal is caused by a coherent rotation, the coercivity is reported to decrease with increasing the angle θ.[31] The angular dependence of coercivity shown in Fig. 2.6 nearly agrees with that calculated by Jacobs,[32,33] in which he assumed the incoherent rotation of magnetization, so called " fanning model ". The coercivity expected from the " fanning model " is about 600 Oe which is close to the measured coercivity of 350 Oe. Thus, the considerably lower coercivity of γ-Fe_2O_3 particles than the value expected from $2\pi I_s$ is considered to be mainly responsible for the incoherent rotation of magnetization.

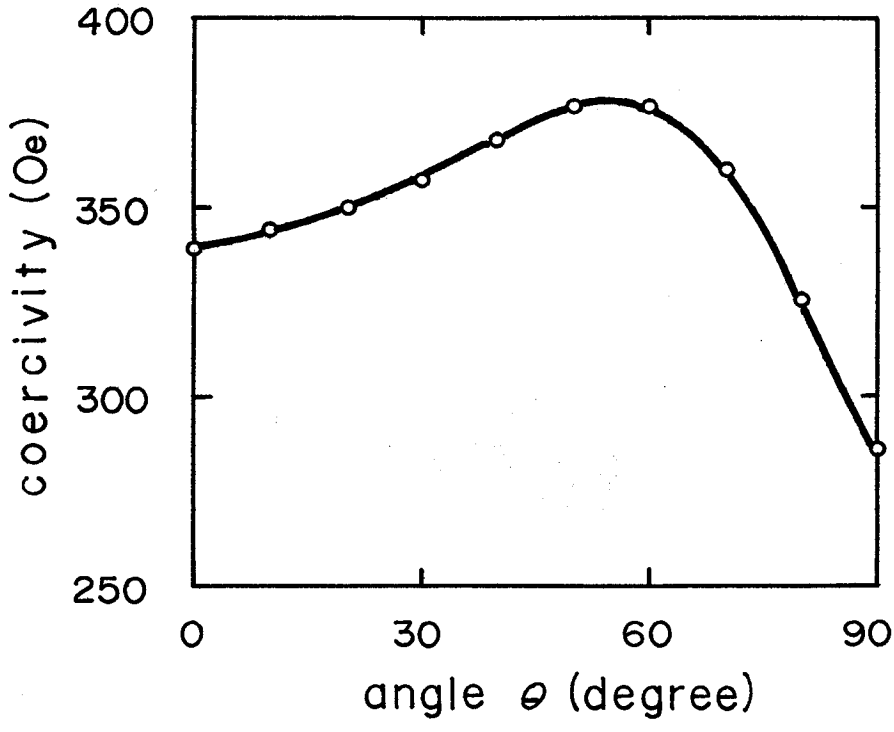

Fig. 2.6 Dependence of coercivity of oriented γ-Fe_2O_3 particles on the angle θ between the direction of orientation and the direction of measurement.

3. Magnetic Properties of Cobalt-Substituted Iron Oxide Partices

3.1. Instability of Magnetic Properties of Cobalt-Substituted Iron Oxide Particles

Acicular γ-Fe_2O_3 particles are widely used as the main material for a recording tape. The magnetic anisotropy of γ-Fe_2O_3 particles is induced by their acicular shape, and γ-Fe_2O_3 particles with a coercivity as high as 470 Oe have been made.[3] However, a magnetic material having higher coercivity is required as a better recording substance. Cobalt-substituted iron oxides were developed for this purpose. The material has the advantage that the coercivity can easily be increased by substituting some small amount of iron with cobalt atoms. However, this material has an unamenable disadvantage that the magnetic properties become unstable not only at high temperature but also during the aging. This temperature and time dependence do appear in the particle coercivity and printing effect. The coercivity gradually increases with a lapse of time even at room temperature, and printing effect becomes significantly large as time gone in the cobalt-substituted iron oxides. These instabilities are believed to be mainly due to the migration of cobalt ions in the spinel lattice as known in iron-cobalt ferrite containing a small amount of cobalt.[35-37]

In our sample preparation it is possible to control the amount of Fe^{2+} ion content in the lattice at any ratio ranging from 0.33 in Fe_3O_4 to zero value in γ-Fe_2O_3. The so-called commercial cobalt-substituted iron oxides are the intermediate oxides between Fe_3O_4 and γ-Fe_2O_3. The existence of Fe^{2+} ions in the particles appears

to be connected with an instability in the coercivity. However, no detailed study has been reported on the subject. In this investigation, the origin of the instability was discussed focusing our attention on the role of Fe^{2+} content in it.[38-40]

3.1.1. Method of Preparation

Particles of γ-Fe_2O_3 with an average length of 0.4 μm, an average acicular ratio of 6, and a coercivity of 420 Oe were used as a starting material to prepare cobalt-substituted iron oxides. The γ-Fe_2O_3 was well suspended in a solution of cobalt sulfate and sodium citrate. Then, this suspension was cooked at 220°C for 3 h in an autoclave. In this hydrothermal treatment, the γ-Fe_2O_3 particles were reduced to Fe_3O_4 particles in co-containing sulfate, and in so doing some cobalt ions were substituted with those of Fe_3O_4. The cobalt content of the resulting cobalt-substituted Fe_3O_4 shows in approximate agreement with the cobalt content of the added cobalt sulfate. Fig. 3.1 and 3.2 show the electron micrographs of the raw γ-Fe_2O_3 particles and the resultant cobalt-substituted iron oxides, respectively. The variation of morphological appearance with respect to the substituting cobalt is not clearly observed. In this experiment, the cobalt-substituted Fe_3O_4 particles with a cobalt content (Co/Co+Fe) in the range of 0.5 to 2.4 wt% were prepared.

To obtain the samples with various Fe^{2+} contents, the cobalt-substituted Fe_3O_4 particles were slowly oxidized in air in the temperature range between 100 and 180°C. The Fe^{2+} and cobalt

Fig. 3.1 Electron micrograph of raw γ-Fe_2O_3 particles.

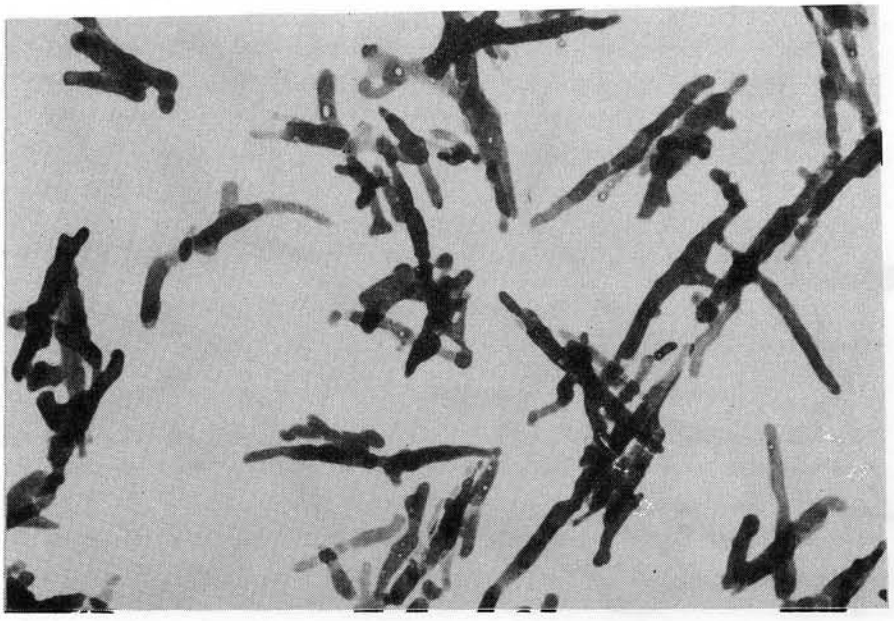

Fig. 3.2 Electron micrograph of cobalt-substituted iron oxide particles.

contents in the samples were determined by means of a chemical analysis.

3.1.2. Effect of Fe^{2+} Content on Variation of Coercivity

Even immediately after the sample preparation the coercivity of the cobalt-substituted iron oxides begins to vary as time gone on. To determine the starting value of coercivity, the samples were at first heated at 150°C for 30 min in an evacuated glass capsule, and then quenched in liquid nitrogen. The coercivity measured at room temperature right after the quenching was assumed as the starting value of the coercivity in this investigation. Table 3.1 is shown both the Fe^{2+} content, the saturation magnetization Is, and the starting value of coercivity Hc. Cobalt content in these samples is 1.8 wt%. The starting value of coercivity is in ranging from 410 Oe to 504 Oe. The coercivity is entirely independent of Fe^{2+} content. The samples were then annealed at a constant temperature of 60°C for 16, 68, 960, and 3620 h respectively. During the annealing, the samples were kept in a evacuated glass capsule. The coercivity was measured at room temperature after each annealing. Fig. 3.3 shows the variation of coercivity obtained when specimen condition is changed as shown in Table 3.1. A similar curves of coercivity variation are seen in all samples except for sample(h). Fig. 3.3 was expressed alternatively by Fig. 3.4 in which the coercivity variation is shown as a function of Fe^{2+} content. As shown in Fig. 3.4, when the samples are annealed for 68 h, the coercivity is found to

Table 3.1 Fe^{2+} content, saturation magnetization Is, and starting value of coercivity Hc of cobalt-substituted iron oxide particles.

sample	a	b	c	d	e	f	g	h
Fe^{2+}/total Fe	0.23	0.19	0.17	0.13	0.10	0.07	0.05	0.01
I_s (emu/g)	83.2	81.2	80.1	78.2	76.5	74.7	73.6	73.2
Hc (Oe) quenched	504	500	496	491	490	489	475	409

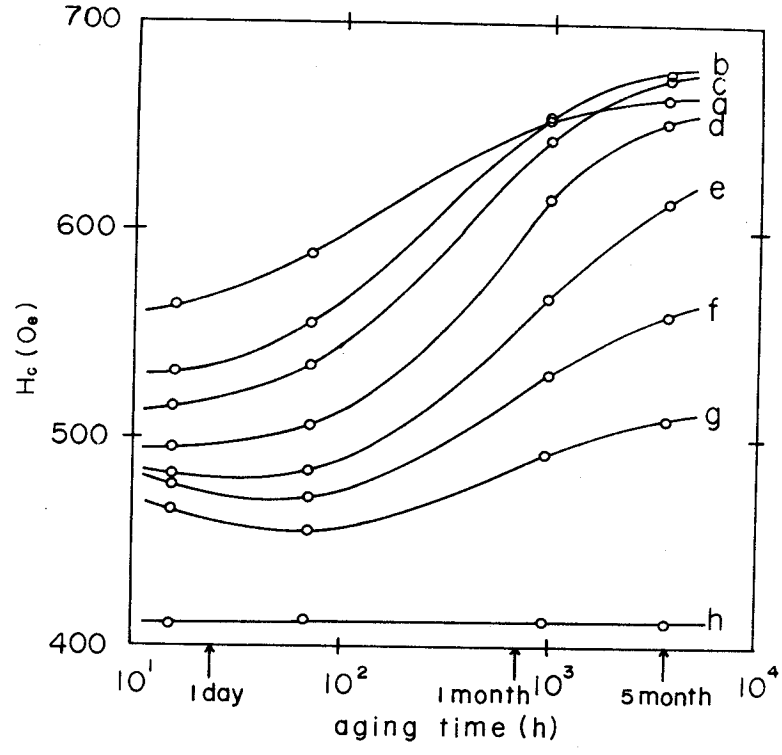

Fig. 3.3 Variation of coercivity to occur in the annealing in the case of cobalt-substituted iron oxides with various Fe^{2+} contents.

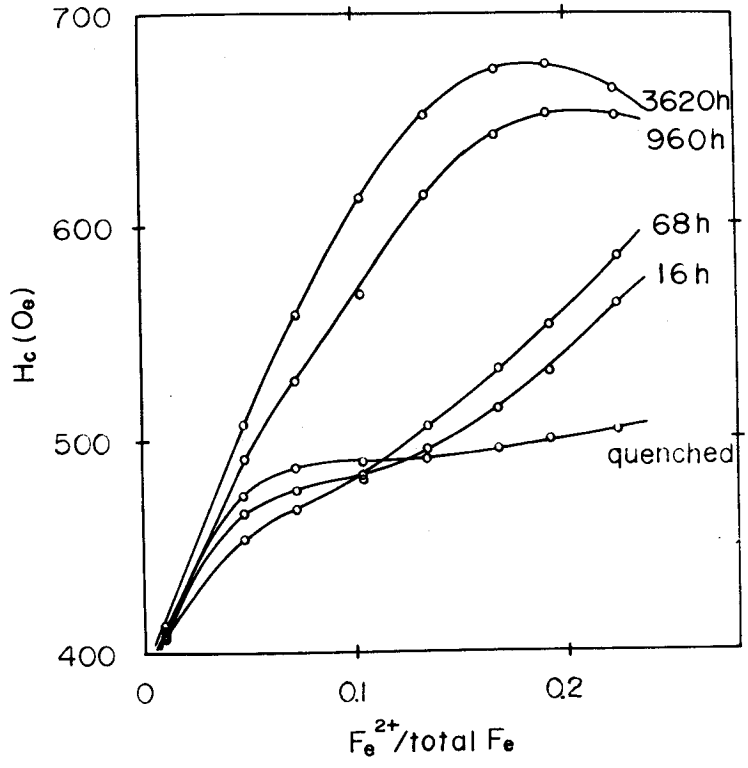

Fig. 3.4 Variation of coercivity as a function of Fe^{2+} content for cobalt-substituted iron oxides. Cobalt content (Co/Co+Fe) is 1.8 wt%.

increase monotonously with increasing Fe^{2+} content. The coercivity of the samples containing less than about 10 wt% Fe^{2+} becomes lower than the starting value after annealing for 68 h. When annealing for 960 h, the coercivity increases remarkably with increasing Fe^{2+} content, and reaches about 650 Oe at 18 wt% Fe^{2+}. The maximum coercivity is found that it exists in the samples whose Fe^{2+} wt% is about 18 and whose annealing duration is about 3620 h. The coercicity of the sample containing 23 wt% Fe^{2+} appears to be close to the saturation value when it is annealed for 3620 h. The coercivity of the sample containing 1 wt% Fe^{2+} does not vary so much even if it was annealed for 3620 h.

3.1.3. Relation between Coercivity and Cobalt Content

The dependence of coercivity on the Fe^{2+} content was examined by using samples containing 0.5, 1.0, 1.6 and 2.4 wt% cobalt. All those samples were heated at 150°C for 30 min, and quenched in liquid nitrogen. the samples were annealed at 60°C for 2160 h. Then the coercivity was measured at room temperature. The result is shown in Fig. 3.5. A similar dependence of coercivity on the Fe^{2+} content is seen in the samples with different cobalt contents. The coercivity increases with the Fe^{2+} content, and it reaches the maximum at the sample containing 18 wt% Fe^{2+}.

Fig. 3.6 shows the relations between coercivity and cobalt content for sample containing Fe^{2+} in the range from 22 to 23 wt% and those less than 1wt%. In the samples containing 22 to 23 wt% Fe^{2+}, the coercivity increases linearly with increasing cobalt

content. The coercivity in the cobalt-substituted iron oxides is mainly due to the shape, crystalline and induced magnetic anisotropy. The linear relation between coercivity and cobalt content suggests that the sum of the crystalline and induced magnetic anisotropy is approximately proportional to cobalt content in the samples containing 0.5–2.4 wt% cobalt. In the samples containing less than 1wt% Fe^{2+}, the coercivity is slightly decreased in the beginning stage of substituting cobalt ion up to 0.5 wt%. But it increases on further substitution.

3.1.4. Measurement of Printing Effect of Particles

When a recorded tape is stored in a cassette reel, the tape has a tendency to magnetize the particles in the adjacent layers up and down by the help of the demagnetizing field of the former layer. This phenomenon is called printing effect. The printing effect is a phenomenon rather difficult to be estimated directly from the printed tape. In order to guess the effect one needs a complicated process. It, on the other hand, is advantageous that the degree of printing effect for particles can be predicted before manufacturing of the recording tape. Hayama reported that the printing effect of recording tape was related to the magnetic annealing effect of particles. The annealing effect was measured using a torque meter.[41] In this investigation, the printing effect of particles was evaluated by measuring the magnetic annealing effect of particles using a vibrating magnetometer.[38] The method is described below. The magnetizing field of one layer of the tape

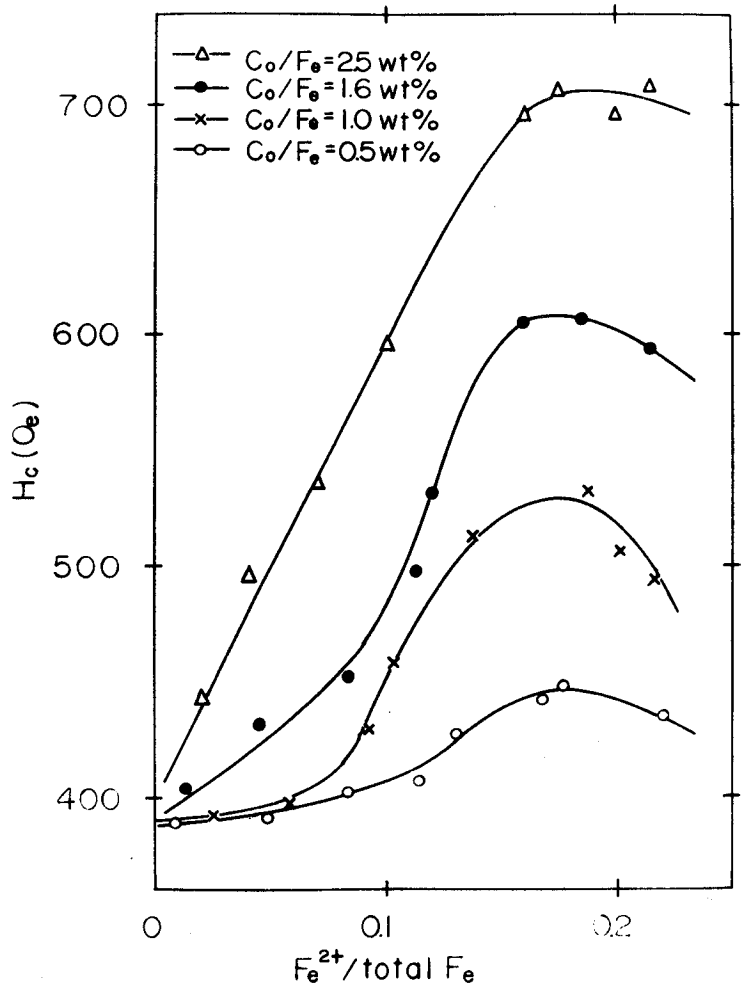

Fig. 3.5 Dependence of coercivity on Fe^{2+} content measured for cobalt-substituted iron oxides with various cobalt contents. Samples were annealed at 60°C for 2160 h.

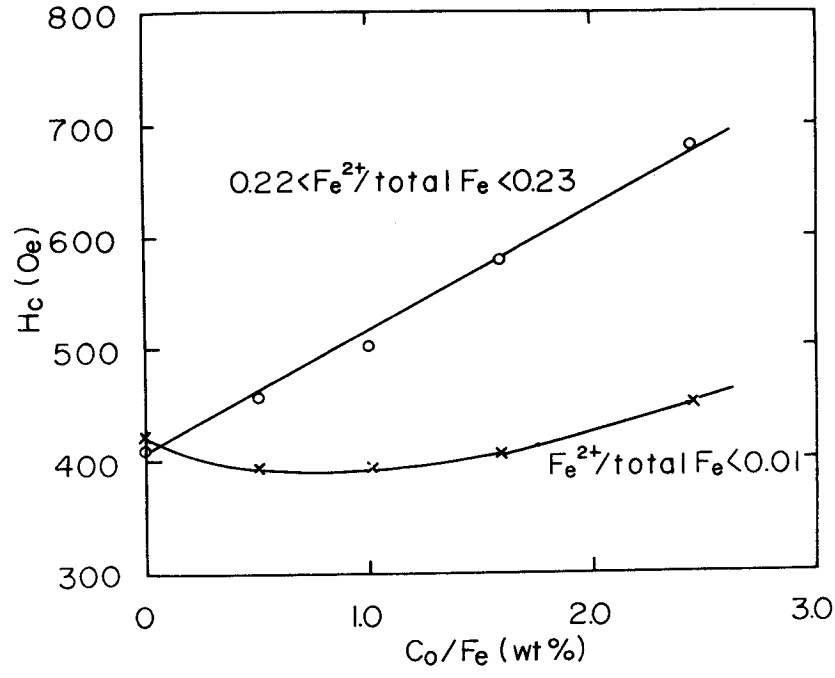

Fig. 3.6 Relation between coercivity and cobalt content in the cobalt-substituted iron oxides containing Fe^{2+} of 22-23 wt% and less than 1 wt%.

to apply upon the adjacent layers is calculated to be about 40 Oe.[41] The magnetic field 40 Oe, therefore, was produced by a helmholtz coil. Then, the particles packed in the vessel with a diameter of 6 mm, and a height of 3 mm was magnetized for a sufficient time by the coil at 60°C. After the magnetization the sample was taken out to room temperature, and the remanent magnetization Irp produced in the sample was measured. The sample, finally, was saturated by the magnetic field of 10 kOe, and obtained saturation remanence Irs was measured. The printing effect was thereafter estimated from the value of -20logIrp/Irs in dB.

3.1.5. Effect of Fe^{2+} Content on Printing Effect

Fig. 3.7(a)-(e) show the relation between -20logIrp/Irs and the duration of magnetizing measured after the annealing at 60°C for the samples given in Table 3.1.[38] Fig. 3.7(a) is shown the result immediately after heating at 150°C for 30 min, and quenching to room temperature. Fig. 3.7(b)-(e) are those measured after annealing for 16, 68, 960 and 3620 h, respectively. In any samples, the decrease of -20logIrp/Irs with increasing magnetizing time is evidently seen. The larger decrease of -20logIrp/Irs is observed in samples containing more Fe^{2+}. The -20logIrp/Irs measured for particles has been compared with the printing effect of recording tape which is manufactured using the same particles. These results indicate that the printing effect of recording tape is predictable when its magnetization time is equal to 80 min. Therefore, in this investigation, $-20\log Irp_{(80)}/Irs$ was defined for the value of

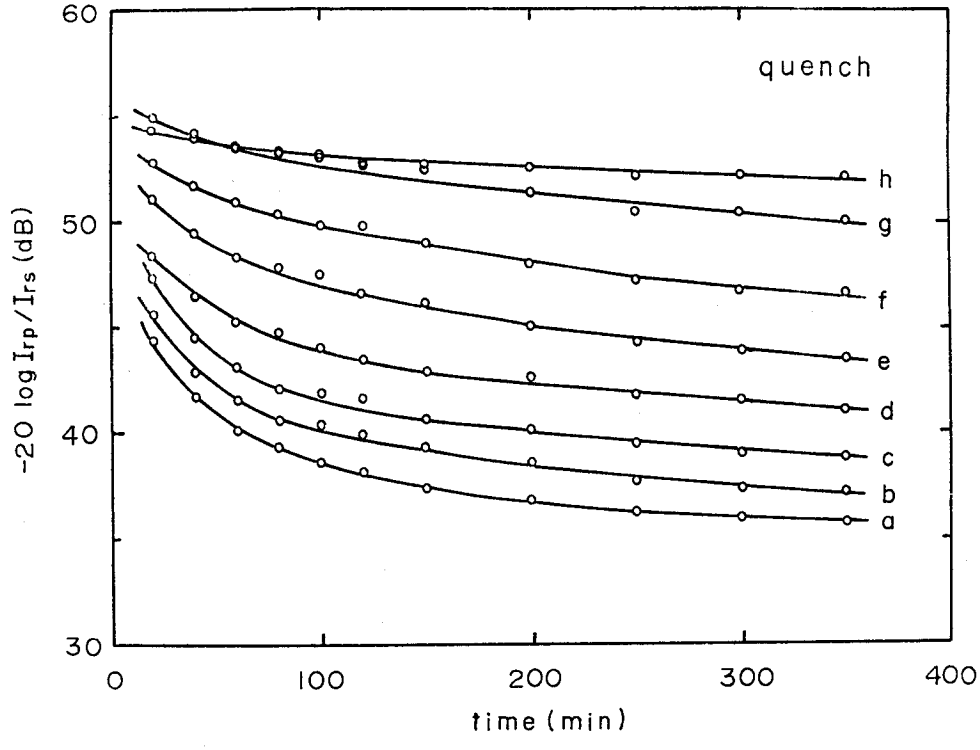

(a)

Fig. 3.7. Relation between -20logIrp/Irs and duration of the applied magnetic field. (a) is the curves for the samples heat-treated at 150°C for 30 min and subsequently quenched, while (b)-(e) are those heat-treated at the same temperature but for different duration of annealing.

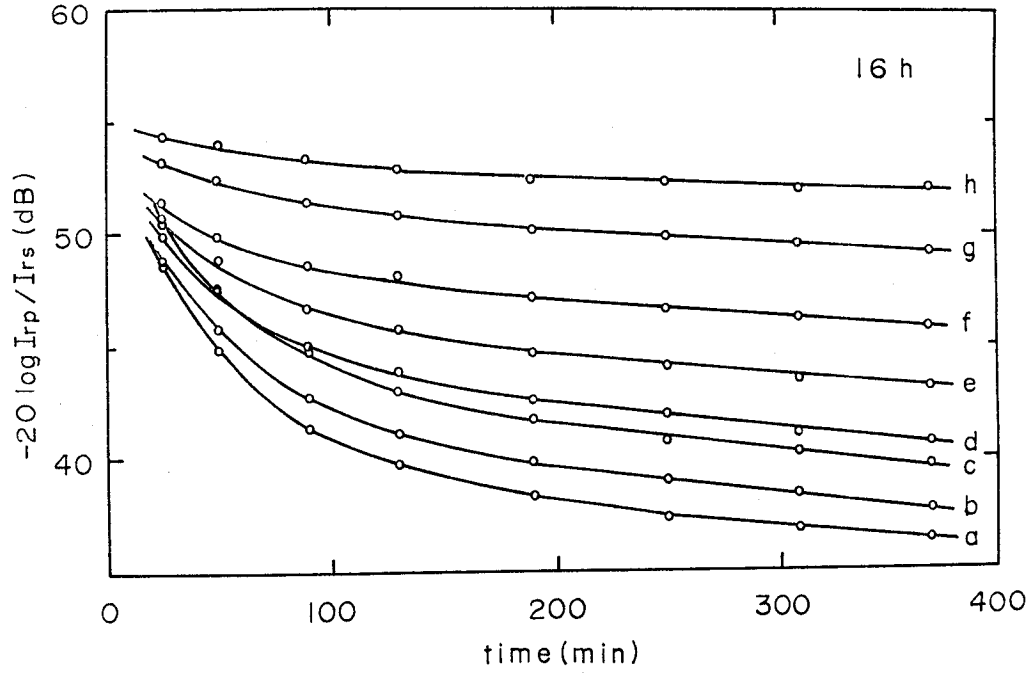
60
50
40
-20 log Irp / Irs (dB)
16 h
h
g
f
e
d
c
b
a
0
100
200
300
400
time (min)

(b)

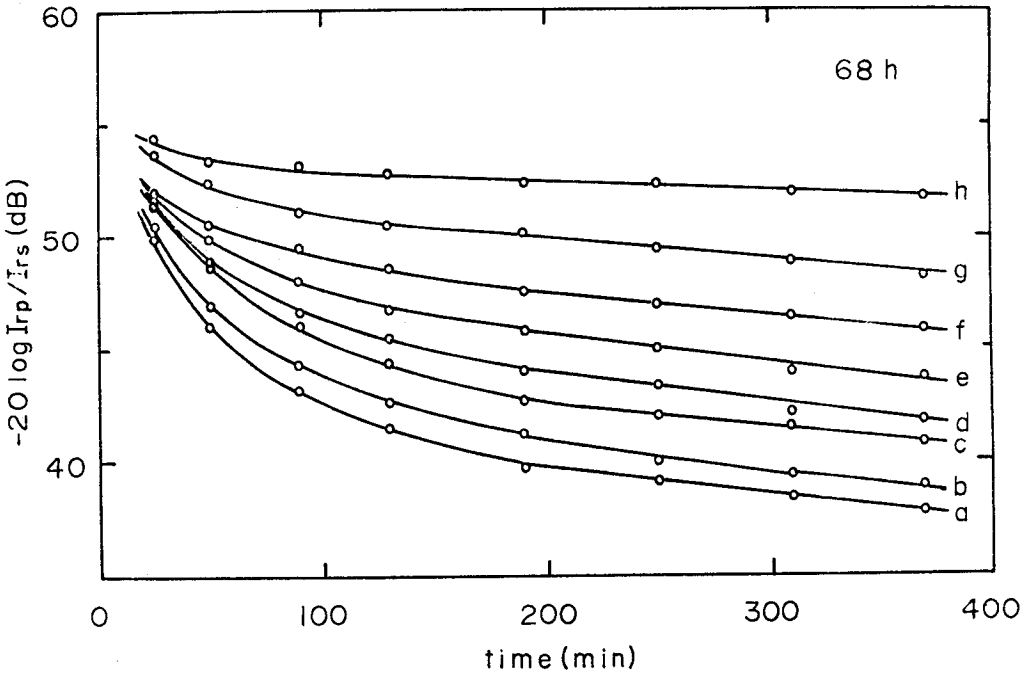
60
50
40
68 h
h
g
f
e
d
c
b
a
-20 log Irp/Irs (dB)
0
100
200
300
400
time (min)

(c)

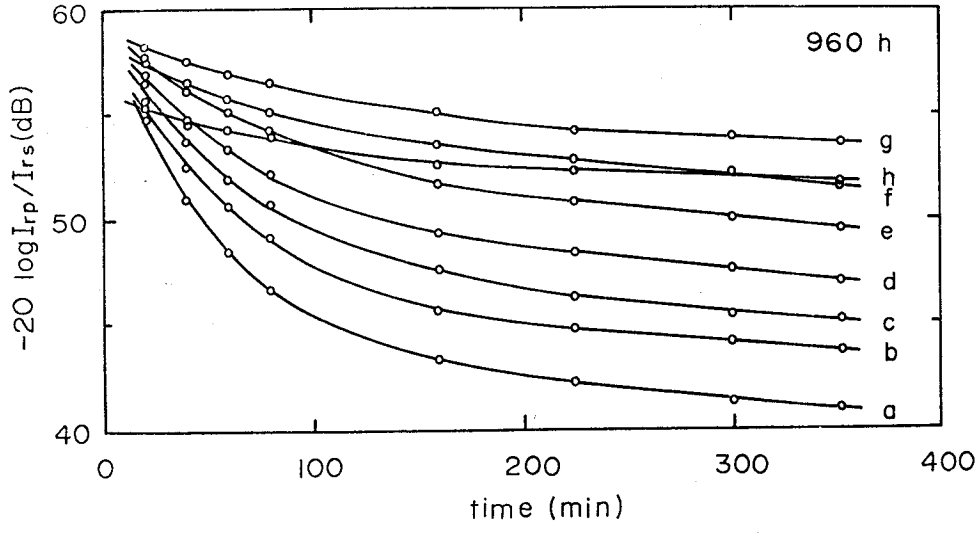
960 h
g
h
f
e
d
c
b
a
60
50
40
0
100
200
300
400
-20 log Irp/Irs (dB)
time (min)

(d)

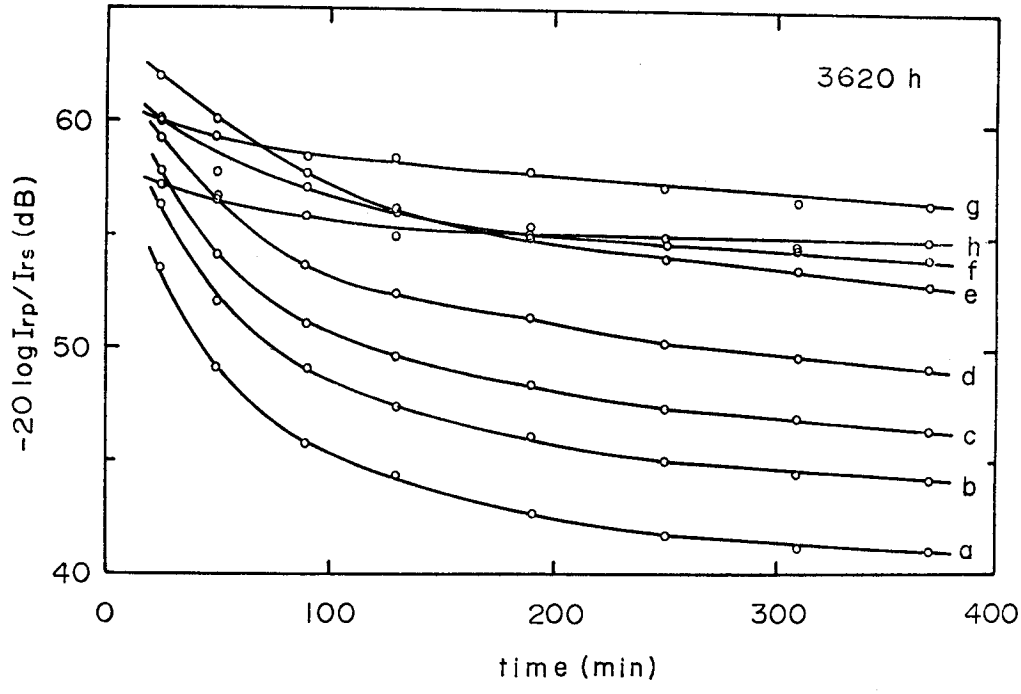
3620 h
60
50
40
-20 log Irp/Irs (dB)
0
100
200
300
400
time (min)
g
h
f
e
d
c
b
a

(e)

printing effect of particles. Fig. 3.8 shows the relation between $-20\log Irp_{(80)}/Irs$ and the coercivity of cobalt-substituted iron oxides with varying concentration of Fe^{2+} and annealing times. For the samples having the same value of coercivity, the $-20\log Irp_{(80)}/Irs$ decreases, and consequently the printing effect becomes significantly increased with decreasing annealing time. For the samples having the same annealed time, $-20\log Irp_{(80)}/Irs$ shows the tendency to decrease with increasing the coercivity. Fig. 3.9 shows the relation between $-20\log Irp_{(80)}/Irs$ and the coercivity measured for γ-Fe_2O_3 particles containing no cobalt. The $-20\log Irp_{(80)}/Irs$ in the case of γ-Fe_2O_3 particles increases with increasing coercivity, and shows the decreasing tendency instead of increasing in the case of cobalt-substituted iron oxides. Fig. 3.10 shows the $-20\log Irp_{(80)}/Irs$ plotted as a function of Fe^{2+} content for cobalt-substituted iron oxides. The samples annealed for 3620 h show the maximum of $-20\log Irp_{(80)}/Irs$ in the neighbourhood of Fe^{2+} content of 6 wt%. In other samples, the $-20\log Irp_{(80)}/Irs$ decreases with increasing Fe^{2+} content. Thus, the printing effect of cobalt-substituted iron oxides increases with increasing Fe^{2+} content.

3.1.6. Discussion

It is well known that iron-cobalt ferrite containing a small amount of cobalt has a magnetic annealing effect.[36,42] This effect has been explained to be caused by the migration of cobalt ions to the stable sites in the spinel B-site to along the direction of the applied magnetic field. As the result of this ion migration,

high uniaxial magnetic anisotropy is induced in the direction of the applied magnetic field. Iida[37] examined the effect of temperature and vacancy concentration on the relaxation time of the migration in $Co_{0.063}Fe_{2.937}O_4$, and observed that the time decreased with both the increasing temperature and the vacancy concentration. It is considered that Fe^{2+} and Fe^{3+} ions exchange the electrons with each other. The electron hopping from Fe^{2+} to Fe^{3+} makes the cobalt ions migration easy by covering the otherwise very high local potential during the migration. Yanase[34] examined the effect of Fe^{2+} content on the relaxation time for Ni-Zn ferrite, and reported that the relaxation time decreased with increasing Fe^{2+} content.

Acicular cobalt-substituted iron oxides are expected to behave as a single-domain. Therefore, the demagnetizing field due to the shape anisotropy is calculated to be about 2600 Oe from the expected value of $2\pi I_s$. The most commercially available cobalt-substituted iron oxides are intermediate oxides between γ-Fe_2O_3 and Fe_3O_4, and a great deal of Fe^{2+} and cation vacancy exist in oxides. The acicular cobalt-substituted iron oxides possess strong shape effect in the induced magnetic anisotropy.[39]

When cobalt-substituted iron oxides are heated at 150°C, the distribution of cobalt ions may change from some ordered-low temperature state to the original randam atomic distribution by the thermal energy. Therefore, one can not expect any induced magnetic anisotropy. When cobalt-substituted iron oxides are annealed at 60°C, the cobalt ions are expected to migrate to the

stable site by the demagnetizing field. The increase of coercivity by annealing is attributed thus to the induced anisotropy caused by the migration of cobalt ions.[40] As shown in Fig. 3.4, the coercivity increases with increasing the Fe^{2+} content. This result indicates that the Fe^{2+} ions facilitate the migration of cobalt ions.[34] On the other hand, the decreasing in the coercivity of the samples containing Fe^{2+} less than about 10 wt% by annealing is a fact difficult to be understood. As shown in Fig. 3.6, a slight increase of coercivity by substituting more than 0.5 wt% cobalt is explained as follows. In the samples containing a small amount of Fe^{2+}, the migration of cobalt ions to the stable sites is difficult. Therefore, little magnetic anisotropy is induced along the long axis of acicular particles. In the samples containing Fe^{2+} less than 1 wt%, the induced magnetic anisotropy appears to make little contribution to the increase of coercivity.

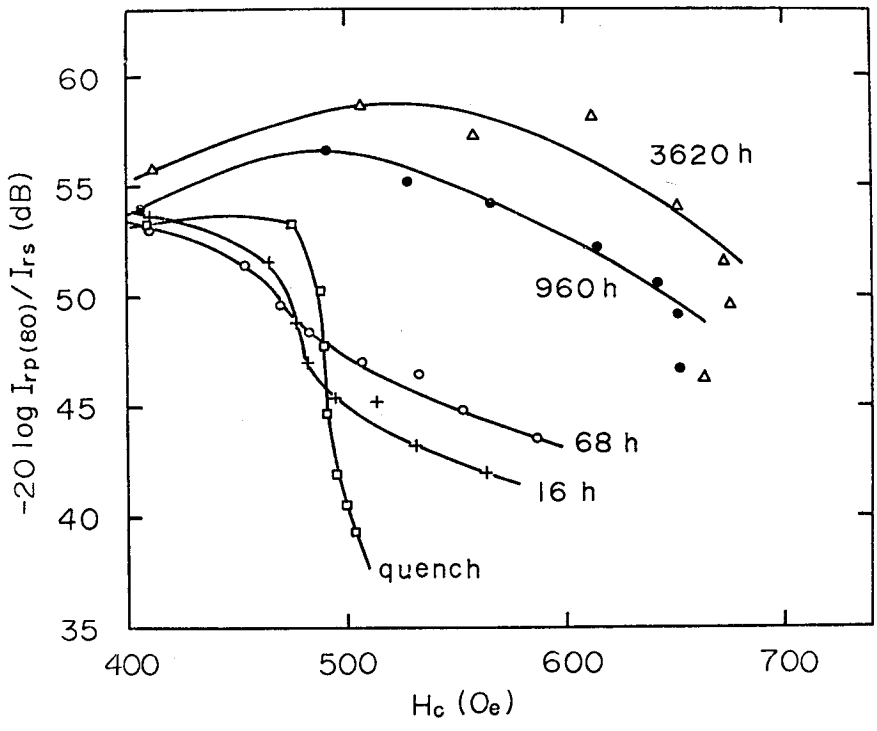

Fig. 3.8 Relation between $-20\log Irp_{(80)}/Irs$ and the coercivity of cobalt-substituted iron oxides with various Fe^{2+} contents and annealing times.

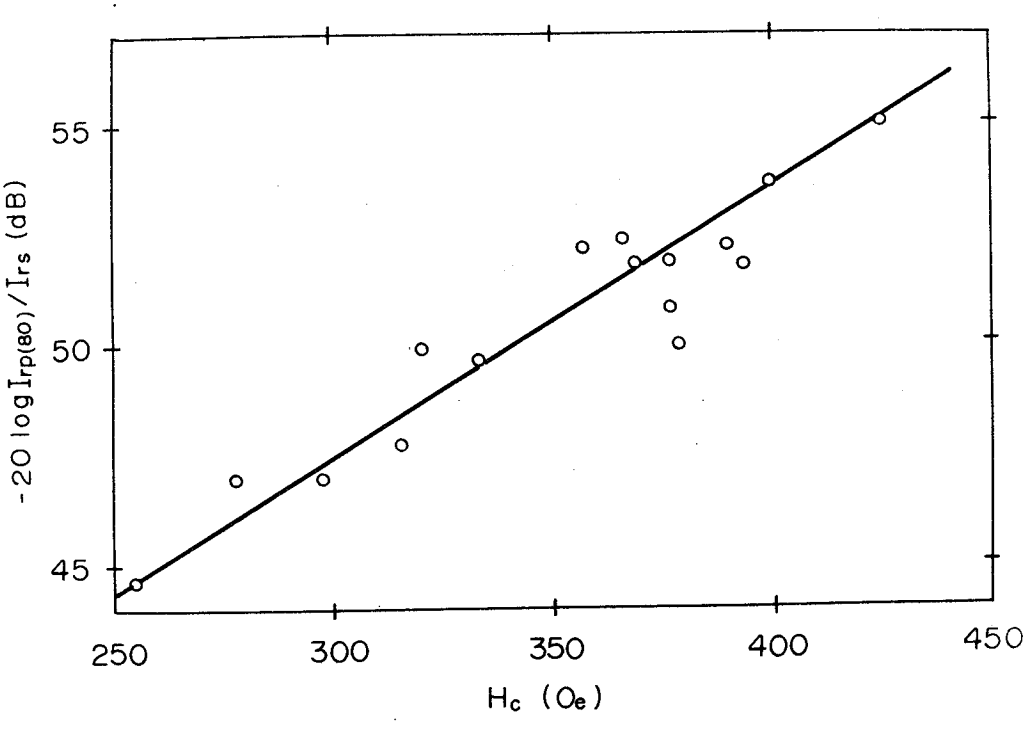

Fig. 3.9 Relation between $-20\log Irp_{(80)}/Irs$ and the coercivity measured for γ-Fe_2O_3 particles containing no cobalt.

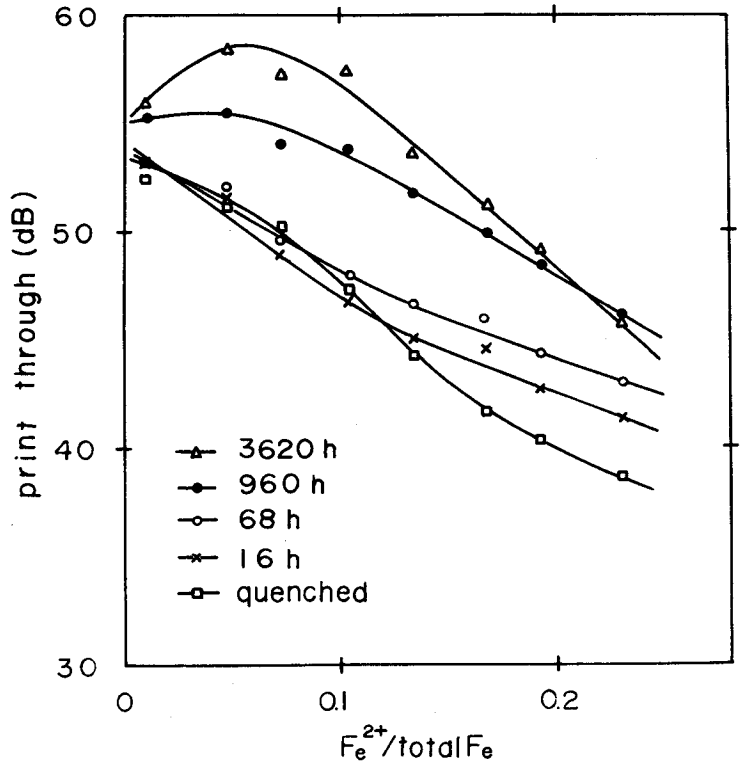

Fig. 3.10 $-20\log Irp_{(80)}/Irs$ plotted as a function of Fe^{2+} content for cobalt-substituted iron oxides with various annealing times.

3.2. Preparation of Crystallized Iron-Cobalt Ferrite and Its Magnetic Properties

An effective method to increase the coercivity of γ-Fe_2O_3 particles is to substitute a small amount of iron ions in γ-Fe_2O_3 by cobalt ions. The most recording tapes prepared from the cobalt-substituted iron oxides have great improvements of recording performance which are deduced from its high coercivity. However, the instability of magnetic properties of cobalt-substituted iron oxides is easily increased in the course of even slowly increasing temperature.[44,45] This instability causes a definite decrease in the output of a recorded signal during prolonged storage. In 3.1, it was shown that the instability was mainly caused by the migration of cobalt ions to stable sites along the direction of demagnetizing field. Here the shape anisotropy can only determine its direction.

To increase the coercivity in γ-Fe_2O_3, iron-cobalt ferrite was crystallized only on the surface of γ-Fe_2O_3 without substituting any iron ion by the cobalt ion. This special method of producing and magnetic properties of the product are described in this section.

3.2.1. Method of Preparation

A cobalt sulfate and a ferrous sulfate were dissolved in water in which are suspended γ-Fe_2O_3 particles having a coercivity of 345 Oe and a suturation magnetization of 74.5 emu/g. The γ-Fe_2O_3 particles play an essential role of seeds on whose surface can be gathered the cobalt and iron ions in question. First the cobalt-iron hydroxides are formed by adding an aqueous solution

of sodium hydroxides in the solution. Then the resultant solution was heated at 90°C for 4 h while it was carefully stirred till iron-cobalt ferrite was formed on the surface of γ-Fe_2O_3. The oxide particles thus made were washed with water and dried at 60°C for 10 h in air.

In the above experiment, a ferrous sulfate was used for a starting material to obtain the particles. If, however, a ferric sulfate was used as a starting material, no significant increase of coercivity from that of raw γ-Fe_2O_3 has been observed. Fe^{2+} and Co^{2+} content in the oxides were determined using chemical analysis.

3.2.2. Variation of Coercivity in Crystallization Process of Iron-Cobalt Ferrite

Nine kinds of samples with nearly constant Fe^{2+} content of 4.5-4.6 wt% and with different molar ratio of cobalt and iron (Co^{2+}/Fe^{2+}) in the range of 0-0.8 were prepared. Fig. 3.11 shows the relation between the coercivity and the Co^{2+}/Fe^{2+} ratio. The coercivity rapidly increases with increasing ratio of Co^{2+}/Fe^{2+}, and in the neighbourhood of the ratio of 0.4, it reaches the maximum with the value of about 620 Oe. Above 0.4 the coercivity of the samples begins to decrease, which continues on increasing the Co^{2+}/Fe^{2+} ratio. This result almost agrees with the report by Bickford[48] who showed that the magnetic anisotropy of the iron-cobalt ferrite represented by $Co_xFe_{3-x}O_4$ showed the maximum value in the neighbourhood of x=0.75.

Fig. 3.12 shows the relation between the saturation magnetization

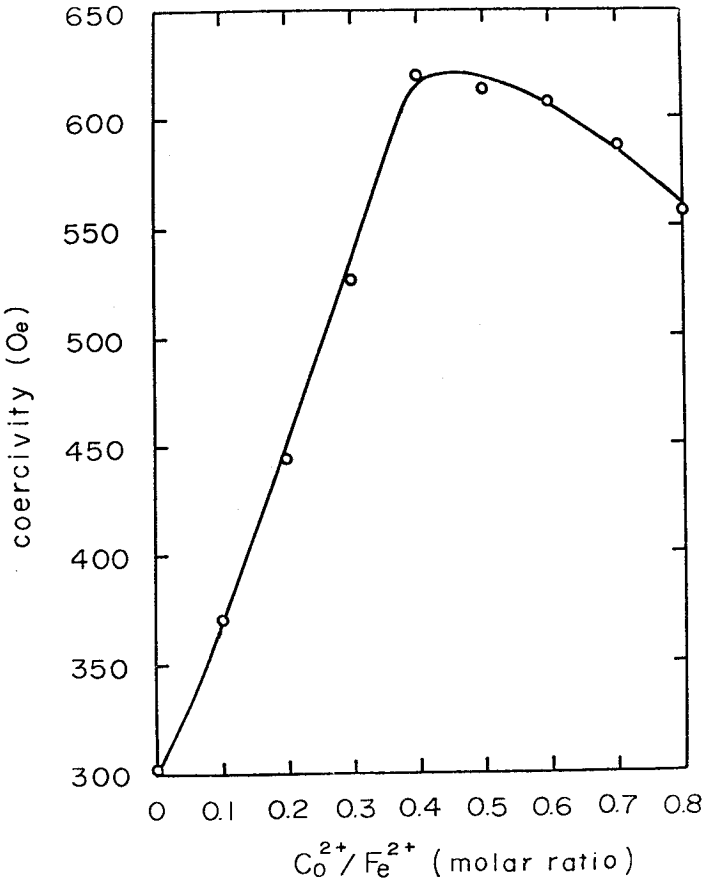

Fig. 3.11 Relation between the coercivity of our iron-cobalt ferrite crystallized on the surface of γ-Fe_2O_3 particles and the ratio of Co^{2+}/Fe^{2+}.

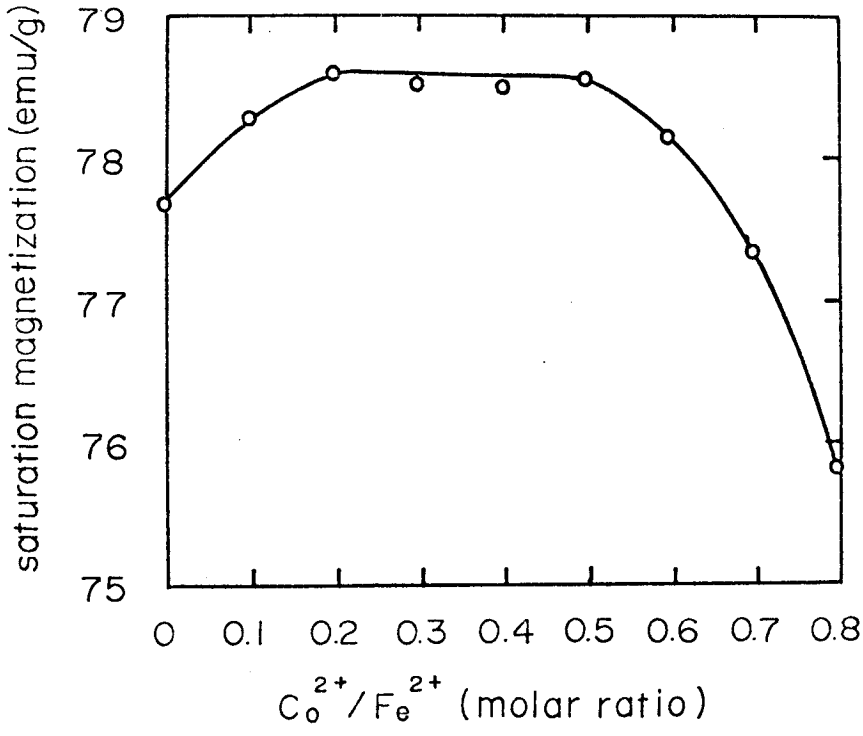

Fig. 3.12 Relation between the saturation magnetization of our iron-cobalt ferrite crystallized on the surface of γ-Fe_2O_3 particles and the ratio of Co^{2+}/Fe^{2+}.

and the ratio of Co^{2+}/Fe^{2+}. The saturation magnetization of the samples with the ratio of Co^{2+}/Fe^{2+} less than 0.6 is in the range of 77.8–78.6 emu/g. The saturation magnetization is independent of the ratio of Co^{2+}/Fe^{2+}. The samples with the ratio of Co^{2+}/Fe^{2+} more than 0.6 show a considerable decrease of the saturation magnetization with increasing the ratio of Co^{2+}/Fe^{2+}. The decrease of the saturation magnetization is expected to be caused by "nonferromagnetic" material such as CoO or $Co(OH)_2$. On the other hand, x-ray diffraction pattern showed only a spinel structure.

3.2.3. Relation between Coercivity and Cobalt Content

Relation between the coercivity and the cobalt content was examined by using the samples having the constant ratio of Co^{2+}/Fe^{2+} of 0.5. The result is shown with (a) in Fig. 3.13. The coercivity increases linearly with increasing the content of cobalt. The sample containing cobalt of 7 wt% shows about 900 Oe. (b) in Fig. 3.13 shows the coercivity of the admixtures of spherical iron-cobalt ferrite particles with an average diameter of 0.5 μm and acicular γ-Fe_2O_3 particles with an average length of 0.5 μm. The coercivities of the spherical iron-cobalt ferrite particles and acicular γ-Fe_2O_3 particles are 1800 Oe and 345 Oe, respectively. The coercivity of the admixtures also increases linearly with increasing the content of cobalt. However, the degree of increase is clearly small compared with that of our iron-cobalt ferrite crystallized on the surface of γ-Fe_2O_3 particles.[47)]

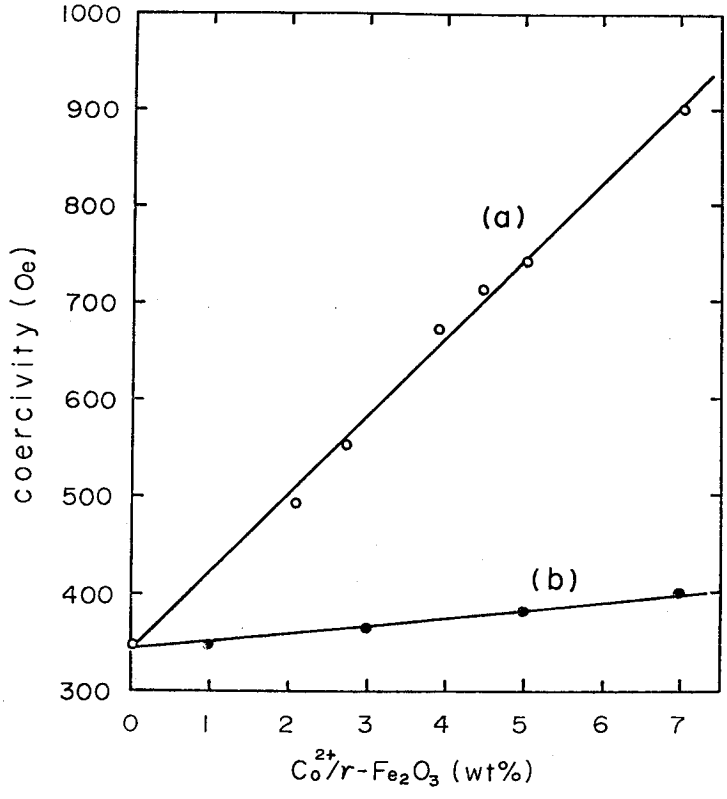

Fig. 3.13 Relation between coercivity and content of cobalt; (a) Our iron-cobalt ferrite crystallized on the surface of r-Fe_2O_3 particles with the ratio of Co^{2+}/Fe^{2+} of 0.5; (b) Admixtures of spherical iron-cobalt ferrite particles having the coercivity of 1800 Oe and acicular r-Fe_2O_3 particles having the coercivity of 345 Oe.

3.2.4. Surface Structure of Iron-Cobalt Ferrite Crystallized on Surface of γ-Fe_2O_3 Particles

In order to confirm the existence of the iron cobalt ferrite on the surface of γ-Fe_2O_3 particles, the oxides with 4.8 wt% of Fe^{2+} and with 0.5 ratio of the Co^{2+}/Fe^{2+} were carefully immersed in dilute hydrochloric acid.[46] After dissolving of a proper weight of the oxides, the cobalt content and the coercivity of the residual oxides were measured. Fig. 3.14 shows the variation of the remaining cobalt content in the residual oxides. The cobalt content rapidly decreases with increasing the dissolved weight. When about 40 wt% of oxides is dissolved, the cobalt content in the residual oxides decreases so small to 0.15 wt%. Fig. 3.15 shows the variation of the coercivity in the residual oxides. By dissolving the oxides only by about 10 wt%, the coercivity of the residual oxides decreases down to 375 Oe. The coercivity of 350 Oe obtained by the dissolving of 40 wt% agrees with that of the raw γ-Fe_2O_3 particles. These results support that the iron-cobalt ferrite crystallizes on the surface of γ-Fe_2O_3 particles, and the increase of the coercivity is entirely attributed to the precipitated iron-cobalt ferrite on the surface of the former.

3.2.5. Variation of Morphology of Particles in Crystallization Process of Iron-Cobalt Ferrite

The process of crystallization of iron-cobalt ferrite was examined with samples having cobalt content of 10 wt% and Co^{2+}/Fe^{2+} ratio of 0.5. The liquid containing Co^{2+}, Fe^{2+}, and γ-Fe_2O_3 particles was heat-treated at 70°C while being stirred.

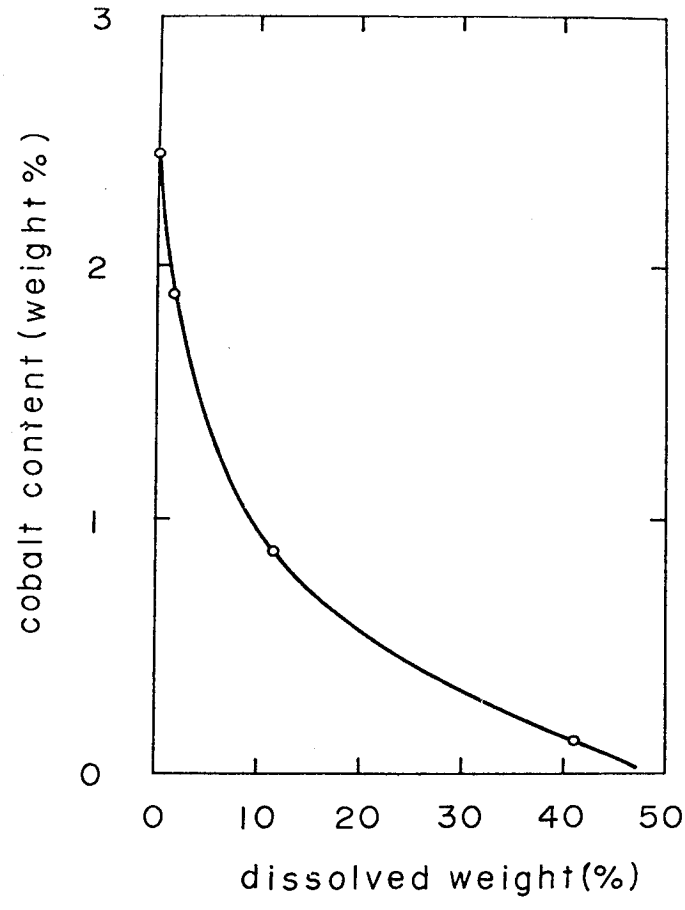

Fig. 3.14 Variation of cobalt content in our iron-cobalt ferrite crystallized on the surface of γ-Fe_2O_3 particles with increasing chemical etching in the hydrochloric acid.

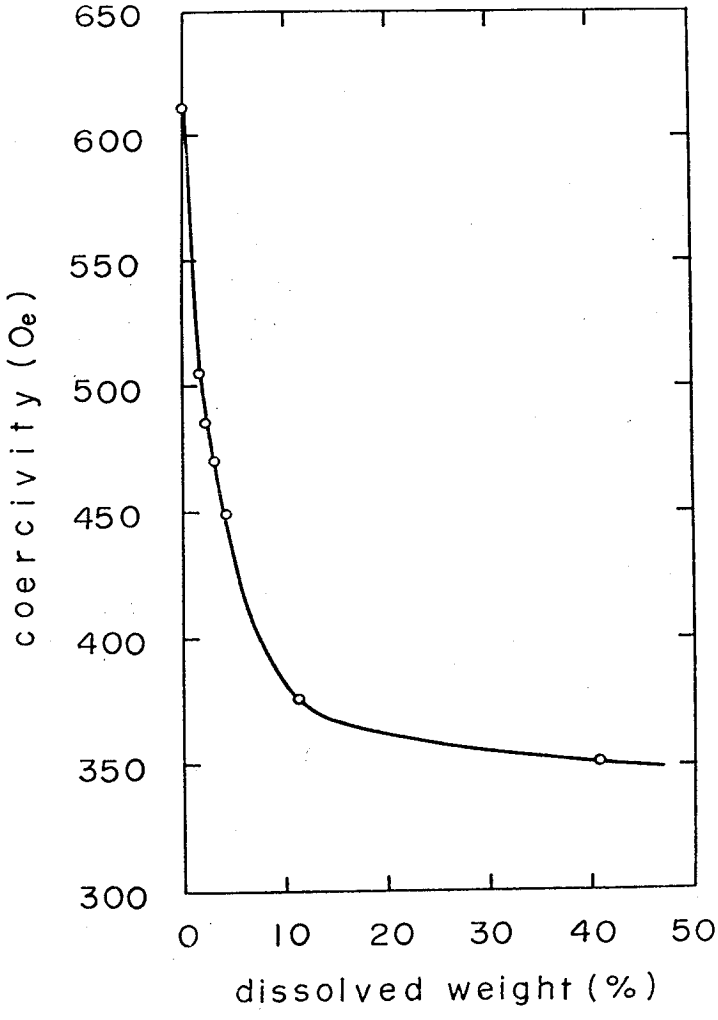

Fig. 3.15 Variation of coercivity of our iron-cobalt ferrite crystallized on the surface of γ-Fe_2O_3 particles with increasing chemical etching in the hydrochloric acid.

Samples were collected after heating for an appropriate time, and the variation of particle morphology and magnetic properties were thus obtained. Fig. 3.16(a)-(d) are the electron micrographs of the samples heat-treated for 0, 30, 90, and 135 min, respectively. In the first photograph, the acicular particles and thin plate-shaped particles are observed. The plate-shaped particles decrease with increasing time of heat-treatment. In the sample heat-treated for 135 min, the plate-shaped particles disappear, and only acicular particles are observed.

In Fig. 3.17 and Fig. 3.18, the coercivity and saturation magnetization of the samples are plotted against the heat-treatment time. Both the coercivity and the saturation magnetization increase with increasing time of the treatment, and at about 150 min, it becomes equal to the value of the saturation. It is considered that the reaction is completed by the heat-treatment for about 150 min. This time of the reaction nearly agrees with the time in which the plate-shaped particles disappear. From these results it is quite likely to assume that the plate-shaped particles, which are considered to be hydroxides of cobalt and iron, are all dissolved, and iron-cobalt ferrite is crystallized on the surface of each γ-Fe_2O_3 particle. The Fe^{2+} content in the resultant oxides nearly agreed with the Fe^{2+} content in the added ferrous sulfate. This implies that the electron exchange between Fe^{2+} and Fe^{3+} occurs on the surface of γ-Fe_2O_3 particles. The squareness in the hysteresis curve of magnetization in our oxides shows only a slight increase, although the coercivity remarkably increases. This suggests that the magnetic anisotropy

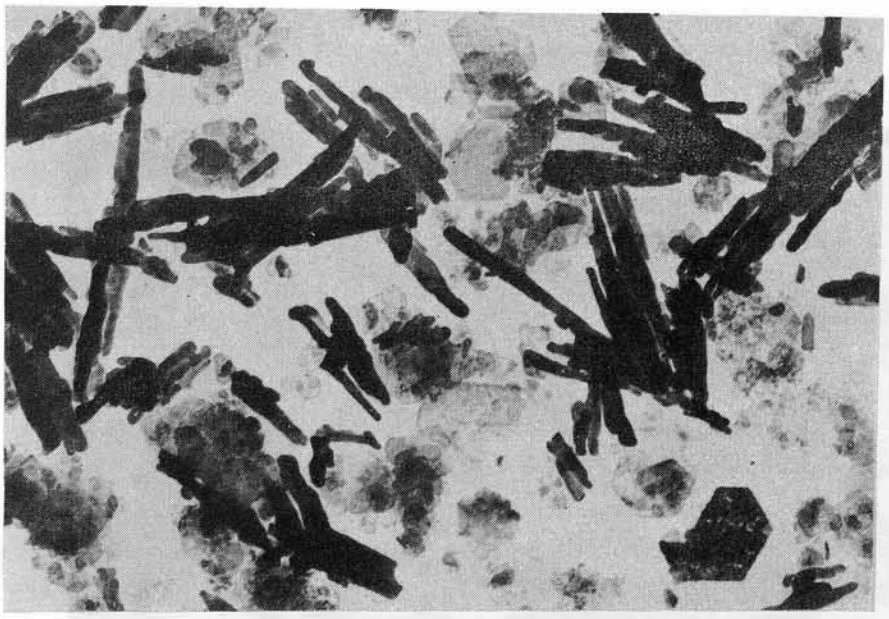

(a)

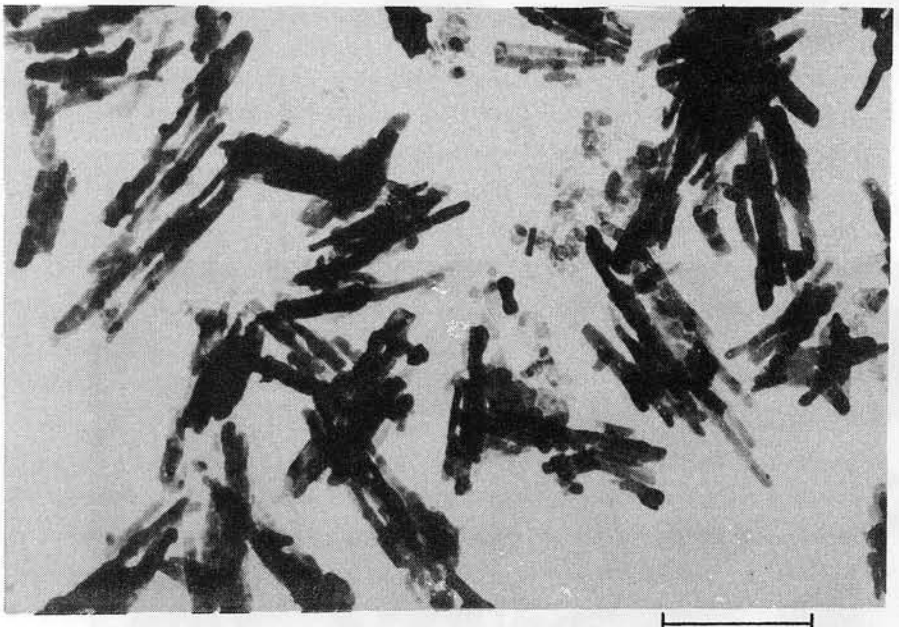

(b)

0.5 μm

Fig. 3.16 Variation of morphology of particles in the process of crystallization of iron-cobalt ferrite to occur in the heat-treatment at 70°C for 0 min (a), 30 min (b), 90 min (c), and 135 min (d).

(c)

(d)

0.5 μm

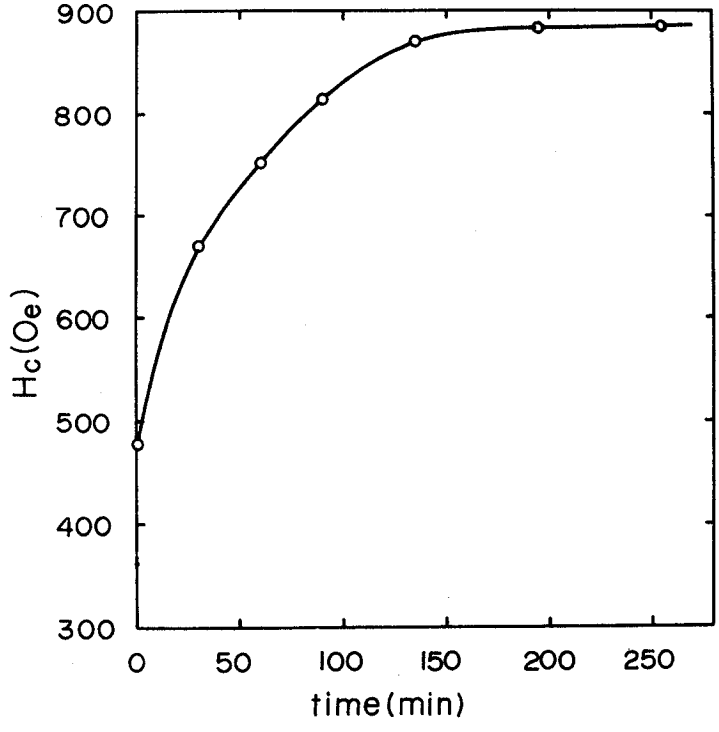

Fig. 3.17 Relation between coercivity of the iron-cobalt ferrite crystallized on the surface of γ-Fe_2O_3 particles and its time of heat-treatment at 70°C.

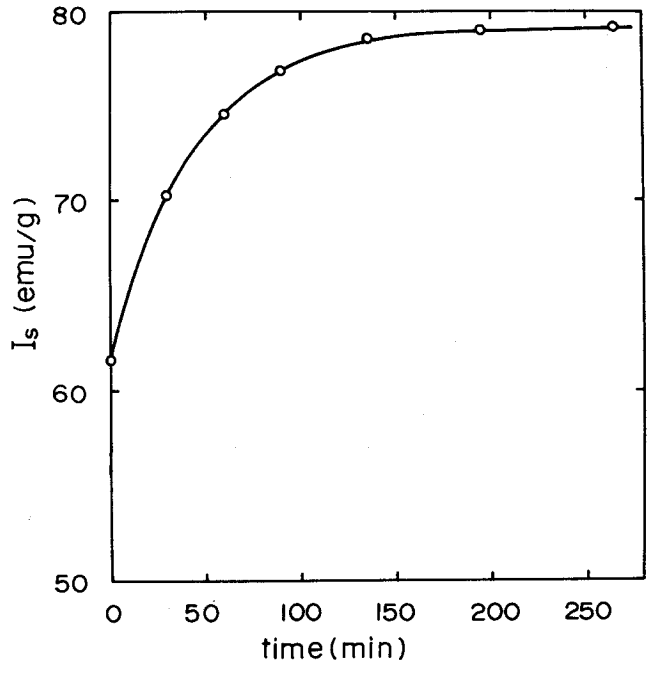

Fig. 3.18 Relation between saturation magnetization of iron-cobalt ferrite crystallized on the surface of γ-Fe_2O_3 particles and its time of heat-treatment at 70°C.

in our oxides is existing nearly in the direction of the elongation of the nuclear γ-Fe_2O_3 particles.

It is expected that γ-Fe_2O_3 particles are reduced to intermediate oxides between γ-Fe_2O_3 and Fe_3O_4 by the electron exchange to occur from the surface of γ-Fe_2O_3, and the iron-cobalt ferrite epitaxially grows on the intermediate oxides which have spinel structure.

3.2.6. Stability of Magnetic Properties

Variation of coercivity occurring in the annealing at 60°C and printing effect in the state of particles were measured for the oxides with cobalt content of 2.6 wt% and with Co^{2+}/Fe^{2+} ratio of 0.5.[47] Fig. 3.19 shows the variation of coercivity in the case of annealing at 60°C after heating at 150°C for 30 min in an evacuated glass capsule. The coercivity after annealing for 5 h is 560 Oe. By annealing for 330 h, the coercivity increases to 565 Oe. The degree of increase of coercivity by the annealing is extremely small compared with that of cobalt-substituted iron oxides described in 3.1.2. Fig. 3.20 shows the printing effect of our iron-cobalt ferrite crystallized on the γ-Fe_2O_3 particles to occur when the cobalt content is changing. $-20\log Irp_{(80)}/Irs$ increases, and consequently the printing effect decreases with increasing cobalt content. The printing effect of our iron-cobalt ferrite is generally small compared with that of cobalt-substituted iron oxides. Such stability of magnetic properties is explainable when one considers that a very high concentration of cobalt ions exist only on the surface of iron oxides, and the migration of cobalt

ions therein is extremely difficult.[49)]

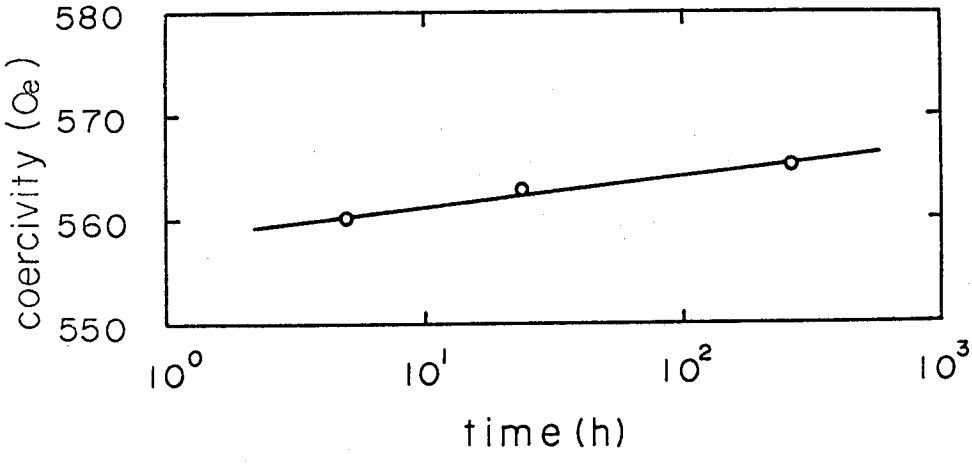

Fig. 3.19 Variation of coercivity with increasing annealing time at 60°C in the case of our iron-cobalt ferrite crystallized on the surface of γ-Fe_2O_3 particles with Co^{2+}/γ-Fe_2O_3 of 2.6 wt% and Co^{2+}/Fe^{2+} ratio of 0.5.

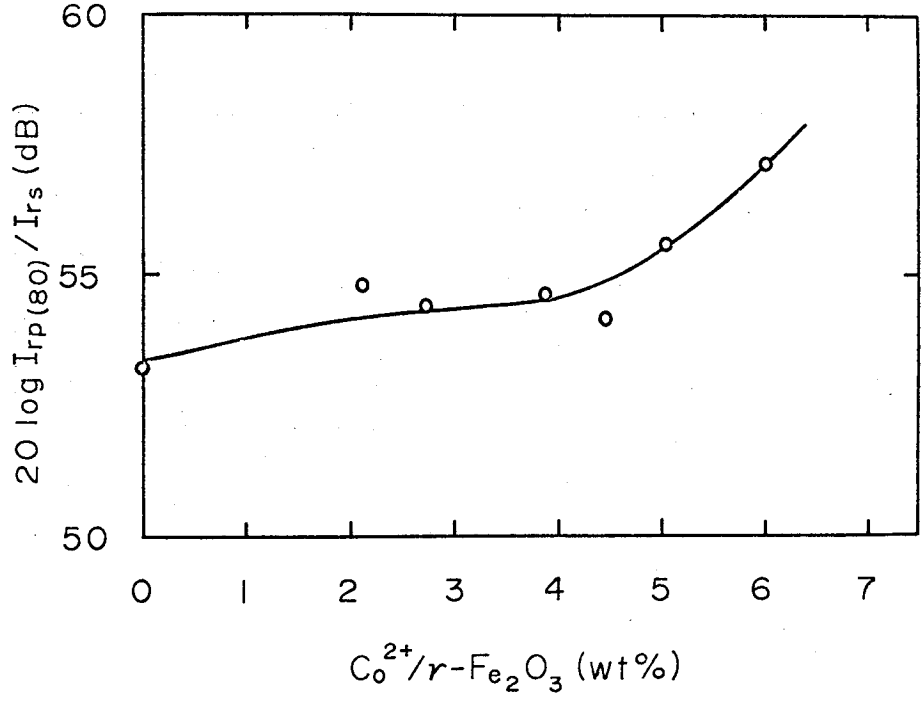

Fig. 3.20 Printing effect of our iron-cobalt ferrite crystallized on the surface of γ-Fe_2O_3 particles having various contents of cobalt.

4. Preparation and Magnetic Properties of MnBi Particles

MnBi is a ferromagnetic compound with the hexagonal NiAs-type structure. This material shows a strong uniaxial anisotropy whose K_1 is equal to 8.9×10^6, K_2 to 2.7×10^6 erg/cm^3, along the c-axis at room temperature.[24,25,50-52] Thin films of MnBi have an easy axis of magnetization perpendicular to the film plane, and have recently been investigated to apply its magneto-optical magnetic writing.[54,55] On the other hand, particles of MnBi have been investigated as a useful material for a permanent magnet since it possesses a very high coercivity.[56-58] Guillaud obtained the coercivity reaching 12000 Oe in the case of 3 μm particles at room temperature.[24] Adams was able to prepare the permanent magnet material called "Bismanol" with the density of 8.1 g/cm^3, Br of 4×10^3 Gauss, the Hc of 7000 Oe, and the (BH) max of 4.3×10^6 Gauss-Oersteds.[56]

Another characteristic property of MnBi is the anomalous temperature dependence of its anisotropy. In spite of the high anisotropy at room temperature, the anisotropy decreases with decreasing temperature, and drops abruptly to zero at 84 K.[24,59,60] Stolz and Shur observed that the coercivity of grains between 3 and 250 μm remarkably decreased at low temperature.[61] This anomalous property of anisotropy suggests a possibility of utilizing the MnBi particles for permanent recording material. That is, signals once recorded at low temperature while its coercivity is being lowered are to be preserved never ever demagnetized at all at room temperature due to the increased coercivity on the following heating. The object of this investigation is to examine the methods to

prepare particles of MnBi having special magnetic properties available for the permanent recording material.

4.1. Preparation of MnBi Particles

4.1.1. Preparation of MnBi

The phase diagram of the Mn-Bi binary system shows that an eutectic reaction occurs at 265°C and a peritectic reaction to form the compound MnBi occurs at 445°C.[62] The conventional method to prepare MnBi compound was as follows. A mixtures of manganese and bismuth were heated in a furnace for about one hour at elevated temperatures (700-1250°C). Each temperature was then lowered to 300-440°C , held there for several hours and reduced finally to room temperature.[56] However, the product obtained by this method consisted of MnBi and unreacted manganese in a matrix of bismuth. In this case further enrichment of MnBi was achieved by a magnetic separation. The final content of MnBi was about 90 percent.[56]

It was reported that a satisfactory MnBi compound with the high-purity was prepared by sintering powders of manganese and bismuth just below a eutectic temperature.[63,64] The sintered-method adopted by Makino[63] is shown below. Manganese and bismuth with purities 99.9 % and 99.5 % respectively were crushed into the size smaller than 200 μm. Then the two admixtures were so mixed well with each other that the manganese composition is 45, 50, 55, 60, and 65 at%. These admixtures were compressed so that they were formed into a molded colum whose diameter and height were

approximately 10 mm and 15 mm respectively. The pressure of 5×10^3 kg/cm^2 was applied. Then, each column was kept in an evacuated glass capsule and heated for 10 days at 265°C which was below the melting point of bismuth. In Fig. 4.1, the saturation values of magnetization at 85 K for these five samples are plotted as a function of manganese content. It is seen that the saturation magnetization becomes the maximum in the neighbourhood of the composition of 55 at% manganese.[65] The saturation magnetization of the samples of 55 at% manganese at 85 K was 79 emu/g, which was about 95 % of the value reported by Heikes.[66] The x-ray diffraction pattern of the samples is shown in Fig. 4.2. Sharp lines of MnBi and faint lines of unreacted manganese are seen.

4.1.2. Preparation of MnBi Particles

In this experiment, the samples of 55 at% manganese was used to prepare particles of MnBi. The sintered block of MnBi was pulverized in a ball mill having steel balls under toluene atmosphere to prevent the oxidation. Four MnBi particles samples with various grades of pulverization with different duration of grinding such as 1, 2, 8, or 24 h were prepared. The electron micrographs of the samples are shown in Fig. 4.3(a)-(d). The distribution of particle size of the sample ground for 1 h is very broad. The sample is composed of plate-shaped particles whose diameter is in the range of 0.1 μm to 0.3 μm and spherical grains with diameter in the range of 0.5 μm to 5 μm. As the grinding advances, many plate-shaped particles were peeled off from one spherical grain. As the result an advanced

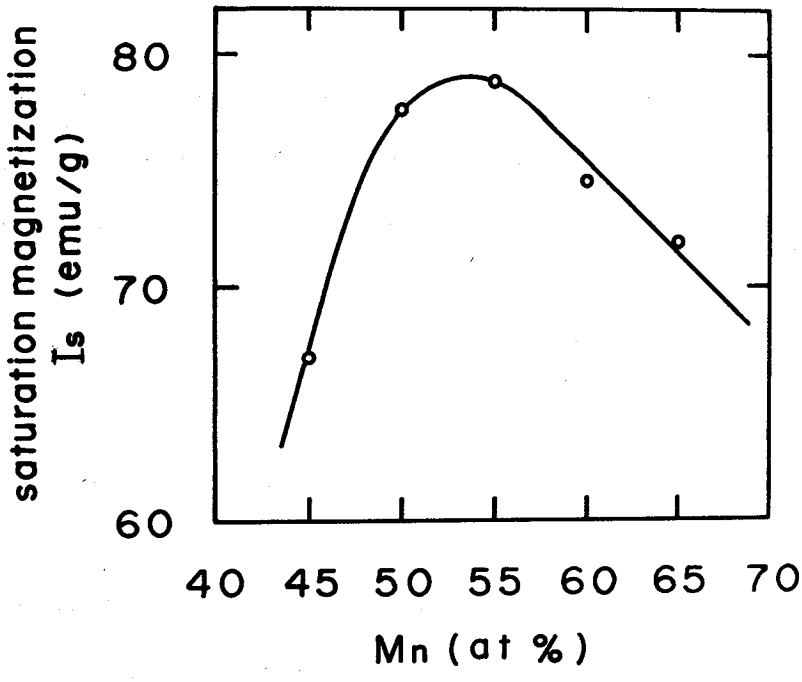

Fig. 4.1 Effect of manganese content on the saturation magnetization in sintered Mn-Bi compounds at 85 K.

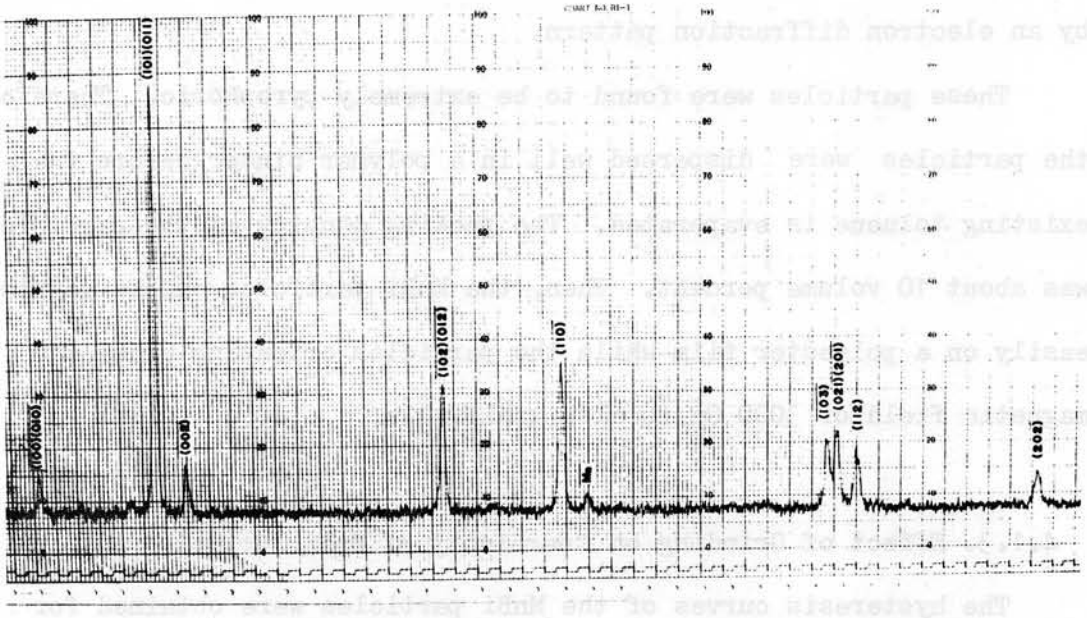

Fig. 4.2 X-ray diffraction pattern of $Mn_{55}Bi_{45}$ compound.

narrowing of the distribution of particle size is observable. The largest particle size of the samples ground for 2 and 8 h are about 3 and 2 μm, respectively. When grinding continued for 24 h, the hexagonal plate-shaped particles were obtained finally. The mean diameter of the plate-shaped particles is less than 0.3 μm, while its mean thickness being 0.01 μm or less. The c-axis was determined to exist in the direction perpendicular to the hexagonal plate plane by an electron diffraction pattern.

These particles were found to be extremely pyrophoric. Therefore, the particles were dispersed well in a polymer binder before the existing toluene is evaporated. The packing density of the particles was about 10 volume percent. Then, the MnBi particles can be painted easily on a polyester film while the particles orienting under the magnetic field of 3000 Oe is also achievable.

4.1.3. Effect of Grinding on Coercivity of MnBi Particles

The hysteresis curves of the MnBi particles were obtained for each sample at temperature of 85 and 300 K up to the maximum field of 16000 Oe. The results obtained are given in Fig. 4.4(a)-(d). For the samples ground for 1, 2, and 8 h, the squareness (remanent magnetization/magnetization under 16000 Oe) at 300 K is found to be about 0.75-0.80. This relatively low value may be responsible for the polycrystal particles occupying still a large volume in the samples. On the other hand, the squareness of the sample ground for 24 h is found to be 0.90 at 300 K. This higher value compared with the other samples suggests that this sample

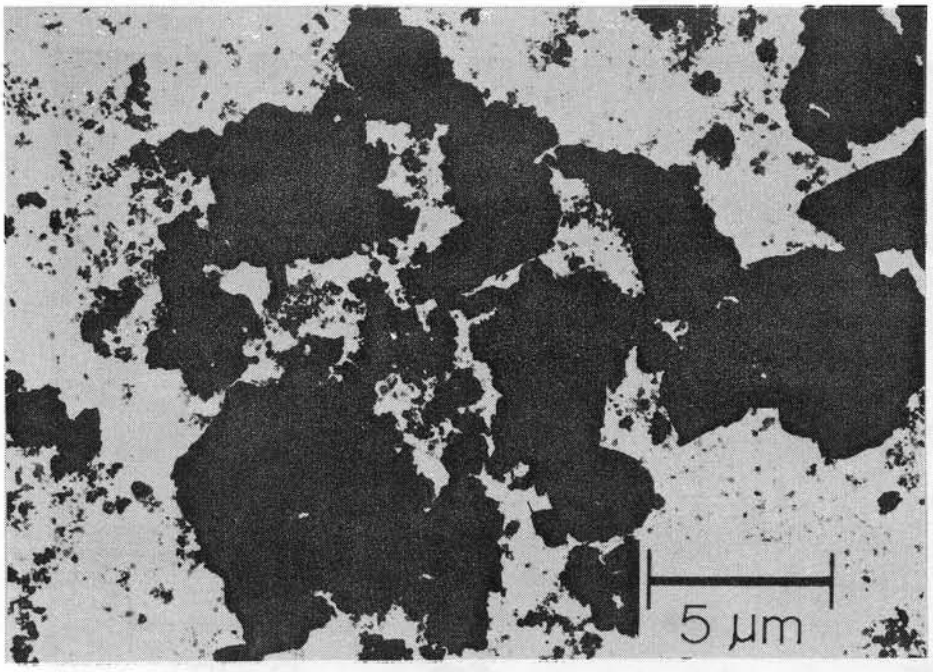

(a)

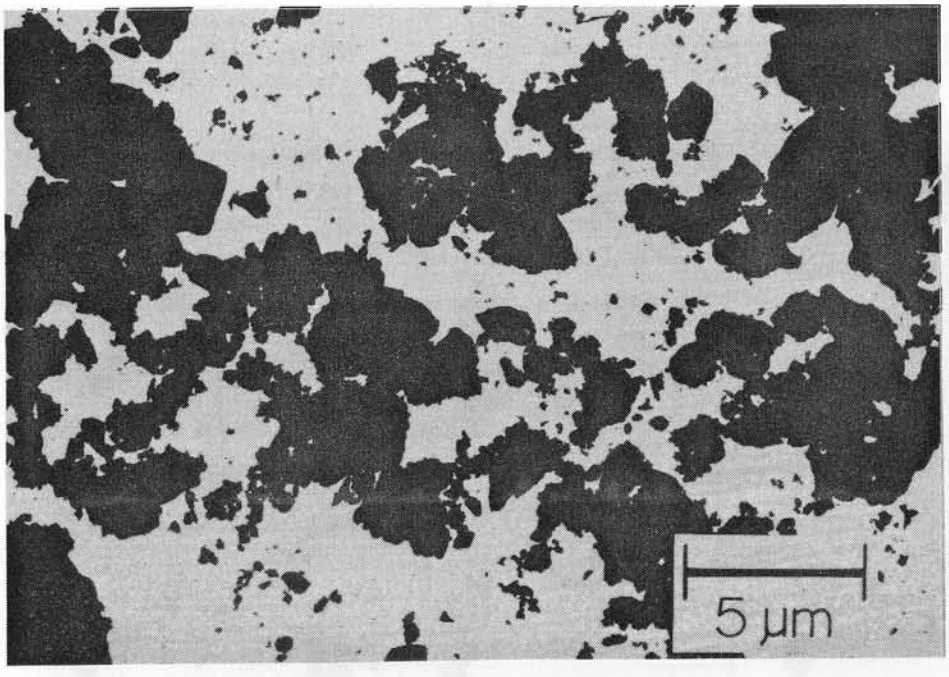

(b)

Fig. 4.3 Electron micrographs of MnBi particles obtained by grinding for 1 h (a), 2 h (b), 8 h (c), and 24 h (d).

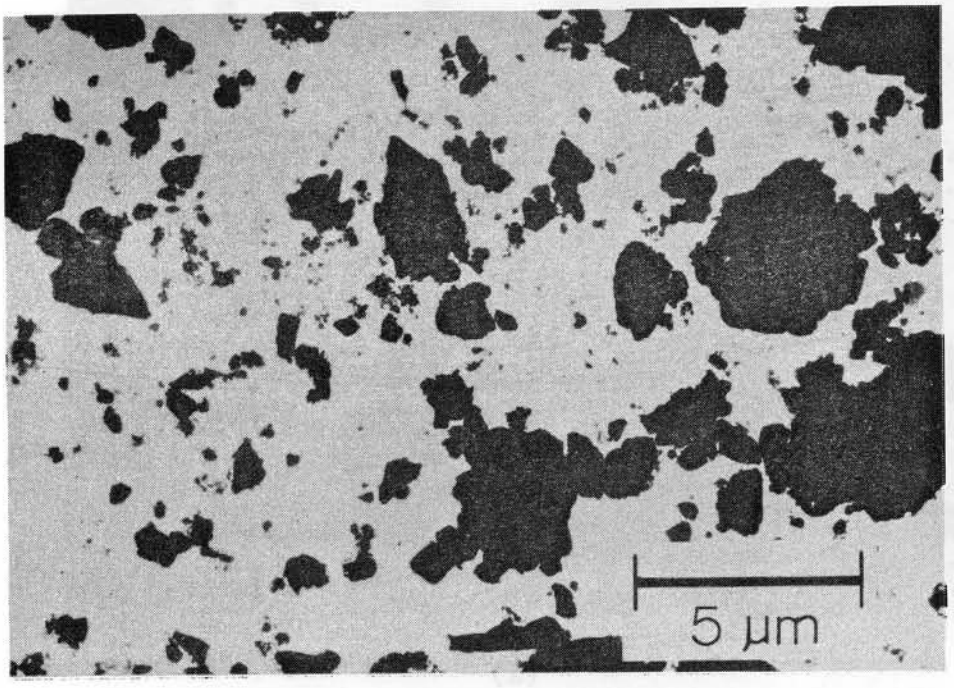

(c)

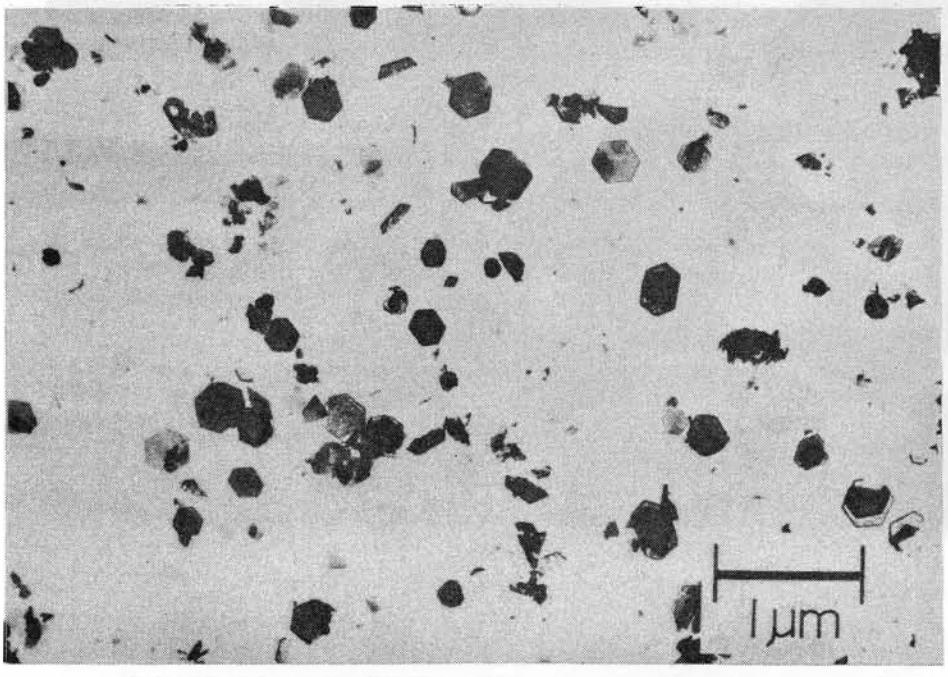

(d)

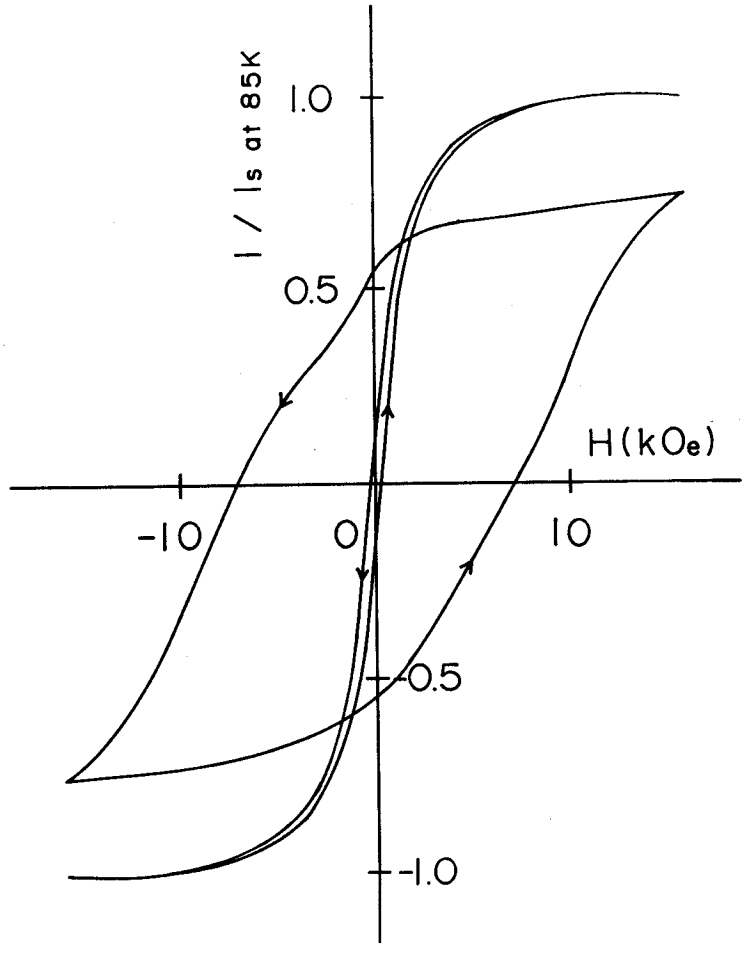

(a)

Fig. 4.4 Hysteresis curves of oriented MnBi particles at 300 K and 85 K. At 300 K, the particles were saturated in the oriented direction, and then the curves were drawn in the maximum field of 16000 Oe. Each curve was measured for the MnBi particles obtained by grinding for 1 h (a), 2 h (b), 8 h (c), and 24 h (d).

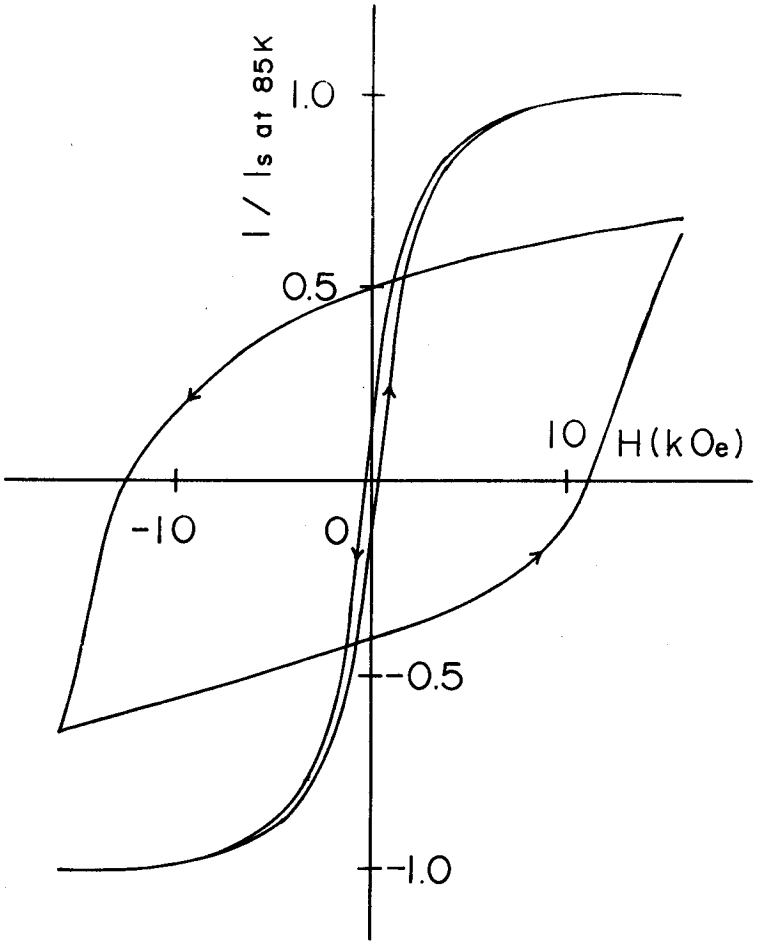

(b)

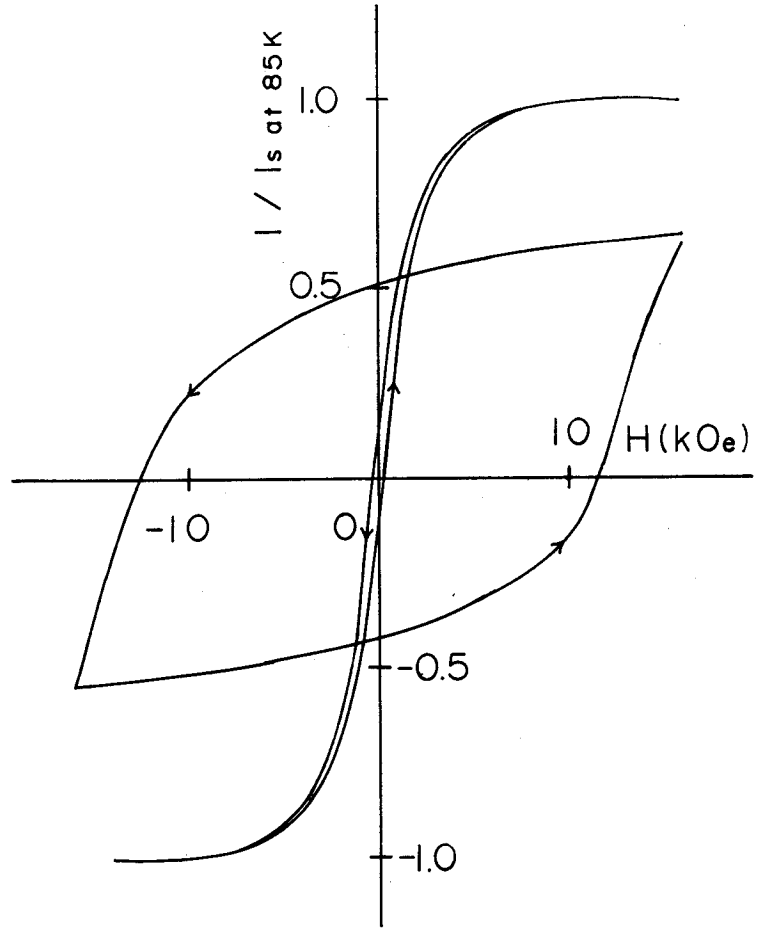

(c)

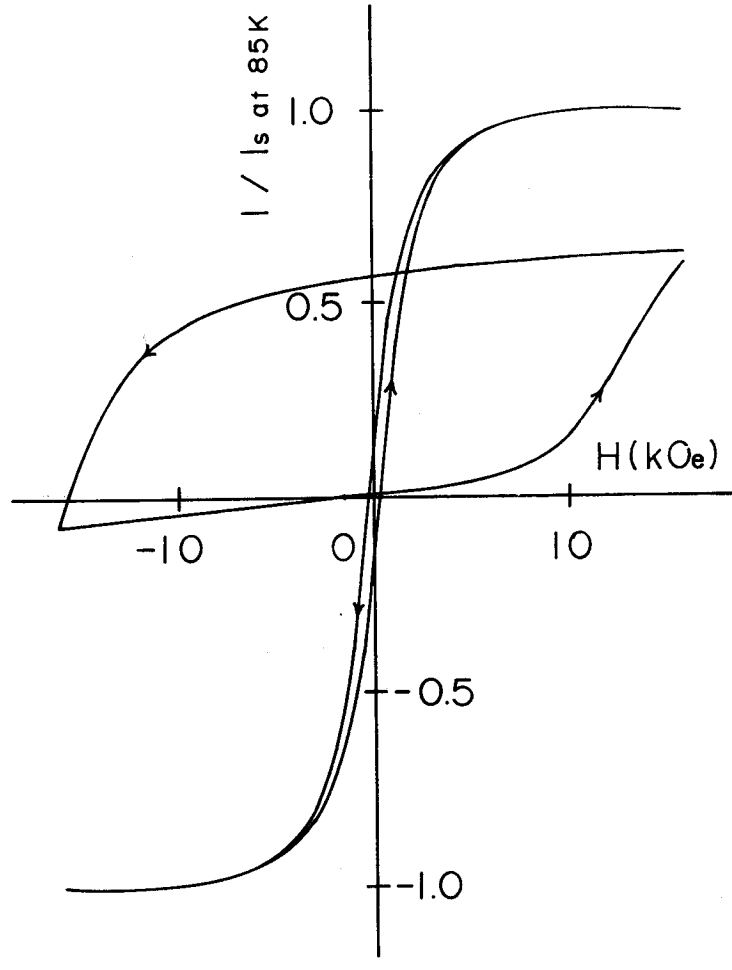

(d)

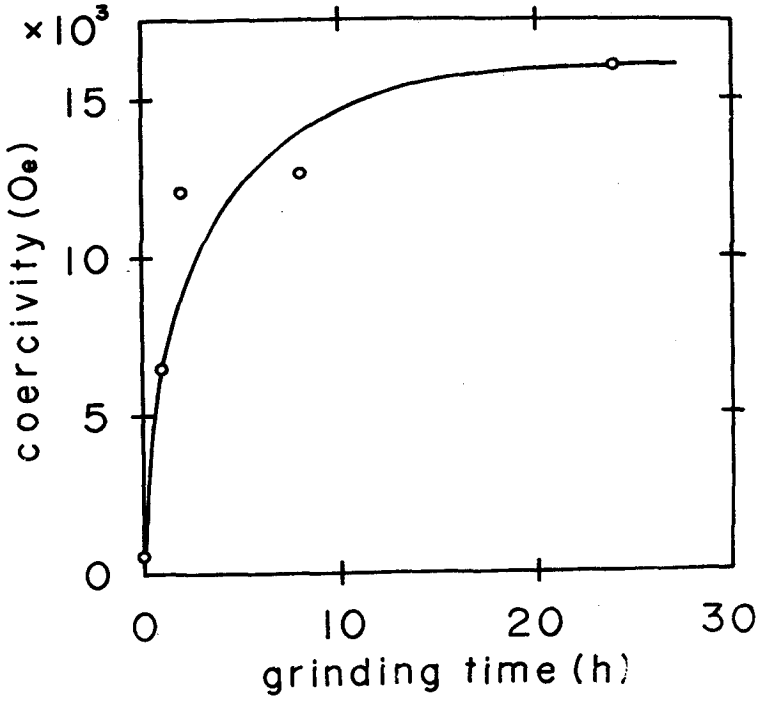

Fig. 4.5 Relation between coercivity of MnBi particles at 300 K and grinding time.

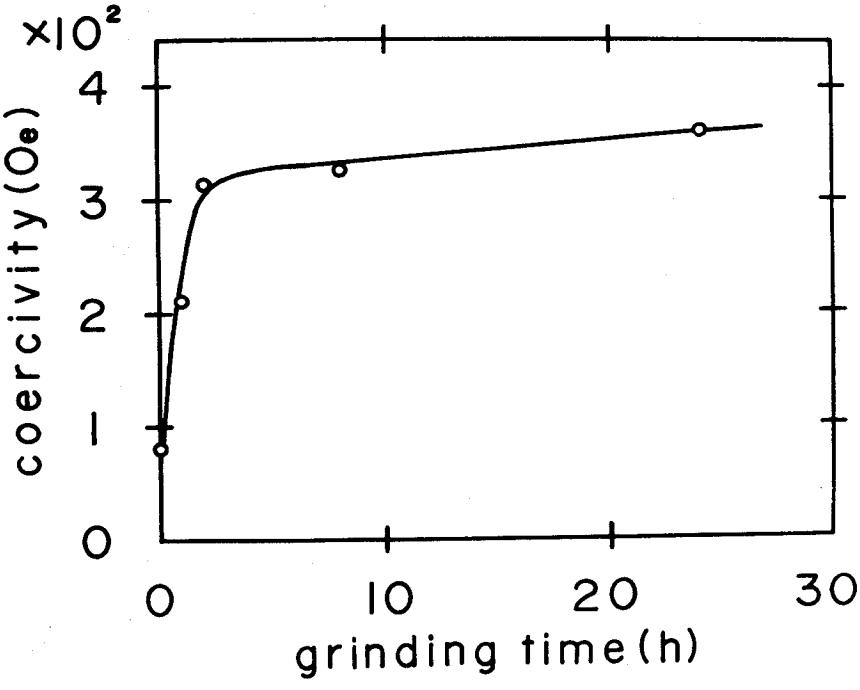

Fig. 4.6 Relation between coercivity of MnBi particles at 85 K and grinding time.

almost consists of single crystals. At 85 K, the squareness of each sample is low, about 0.10–0.15, and almost independent of grinding time.

The coercivity at 300 K and 85 K determined from the hysteresis curves is plotted sa a function of grinding time in Fig. 4.5 and Fig. 4.6, respectively. At 300 K, the coercivity increased remarkably by grinding. The coercivity of the sintered MnBi was only 550 Oe. By grinding for 1 h, the coercivity increased to 6500 Oe. By grinding for 2 h and 8 h, the coercivity increased to 12200 Oe and 12800 Oe, respectively. When the grinding was continued for 24 h, the coercivity reached 16000 Oe. At 85 K, the coercivity of each sample was low compared with that at 300 K, about 80–400 Oe. The low squareness and coercivity at 85 K demonstrates that the crystalline anisotropy of MnBi is very high at 300 K ($K=11\times10^6$ erg/cm^3), but decreases rapidly with decreasing temperature and becomes nearly zero at 85 K.

4.2. Magnetic Properties of MnBi Particles

4.2.1. Temperature Dependence of Coercivity

A temperature dependence of coercivity was measured on platelet-shaped particles shown in Fig. 4.7, which have the diameter from 0.1 to 0.5 μm, and the thickness of 0.01 μm or less.[67] These particles were aligned in polymer binder in the direction of c-axis. The results are given by a solid curve in Fig. 4.8. The coercivity decreases monotonously with decreasing temperature down to about 180 K. Below about 180 K, the coercivity, about 300–600 Oe, is

almost independent of temperature. When the direction of external magnetic field is parallel to the c-axis, the coercivity of the platelet-shaped particles of single-domain is expected to be given by $Hc=2K/Is-4\pi Is$. A dotted curve in Fig. 4.8 shows the calculated curve of the temperature dependence of the coercivity using the above equation. In this calculation, the values for K and Is reported by Guillaud[24] and Heikes[66] were used. When the temperature is above about 180 K, the good agreement of the temperature dependence of coercivity between experimental results and calculation values is seen.

Fig. 4.9 shows the temperature dependence of the squareness measured along the oriented direction. Below about 180 K, the rapid decrease of the squareness is seen.

These results may be taken as an indication that the MnBi particles in this sample are nearly of the critical size of 0.5 μm exhibiting single-domain behavior. However, the observed coercivity of 16000 Oe at 300 K is considerably lower than the calculated value of 23000 Oe. The defects introduced into the particles by grinding may be responsible for the lower coercivity.

4.2.2. Temperature Dependence of Remanence

The critical particle diameter of MnBi particles exhibiting single-domain behavior is expected to decrease with decreasing temperature. Therefore, when MnBi particles of the size close to critical diameter are cooled to lower temperature, the remanence of MnBi particles will decrease rapidly due to the change from single-

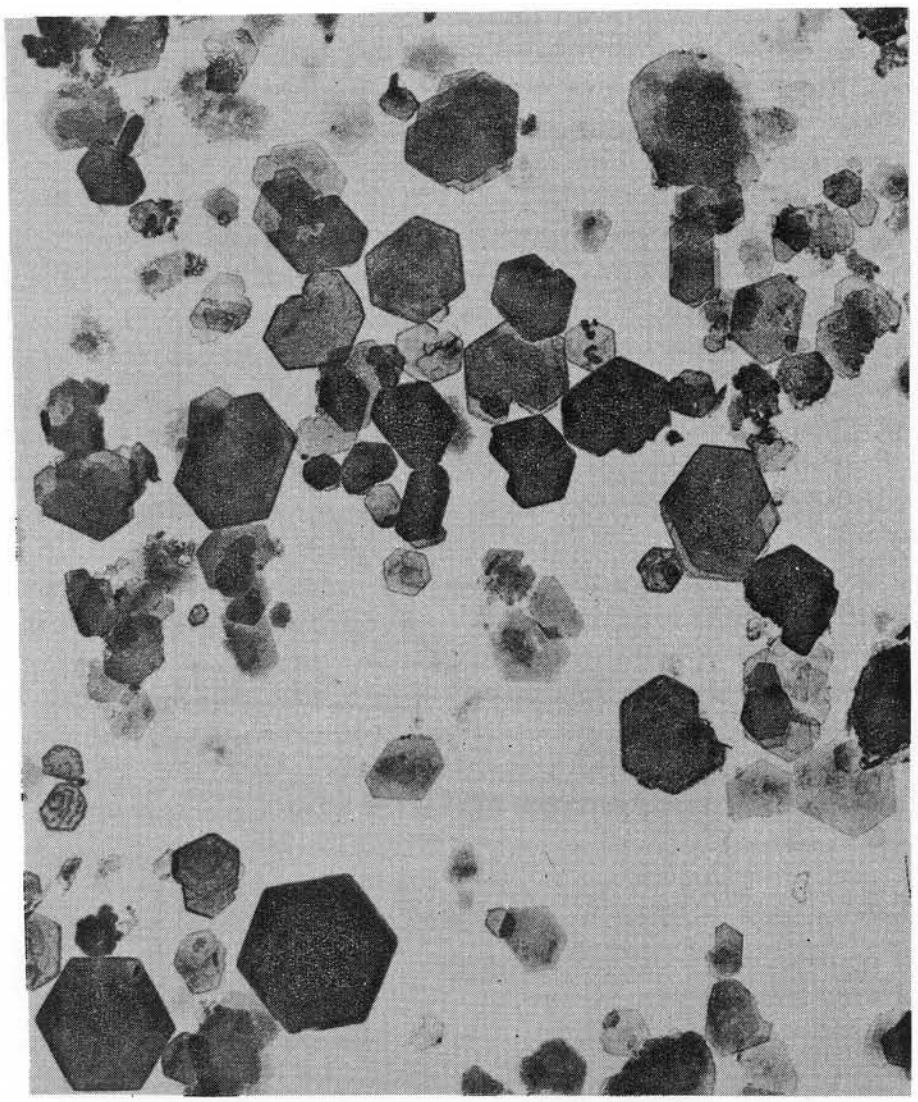

Fig. 4.7 Electron micrograph of MnBi particles.

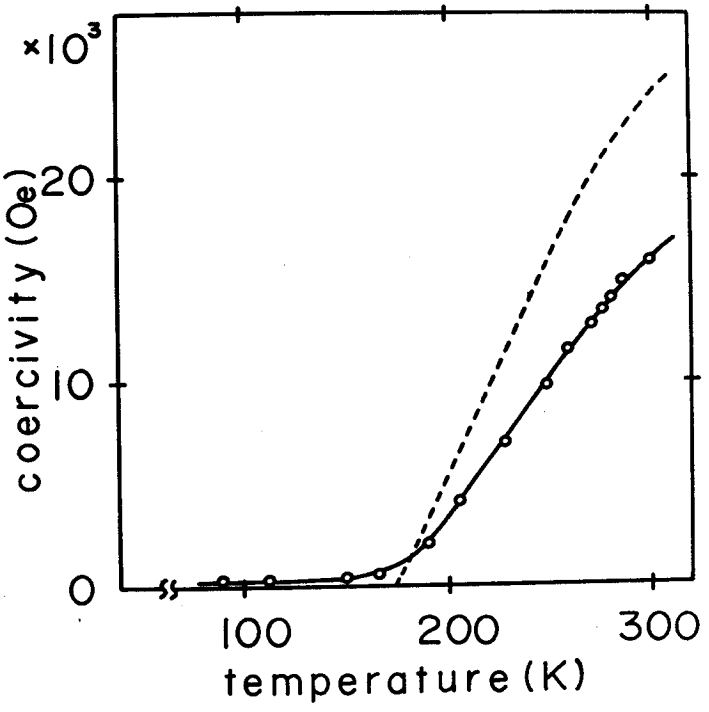

Fig. 4.8 Temperature dependence of coercivity. Solid curve is the coercivity of the oriented MnBi particles. Dotted curve was calculated from $Hc=2K/Is-4\pi Is$.

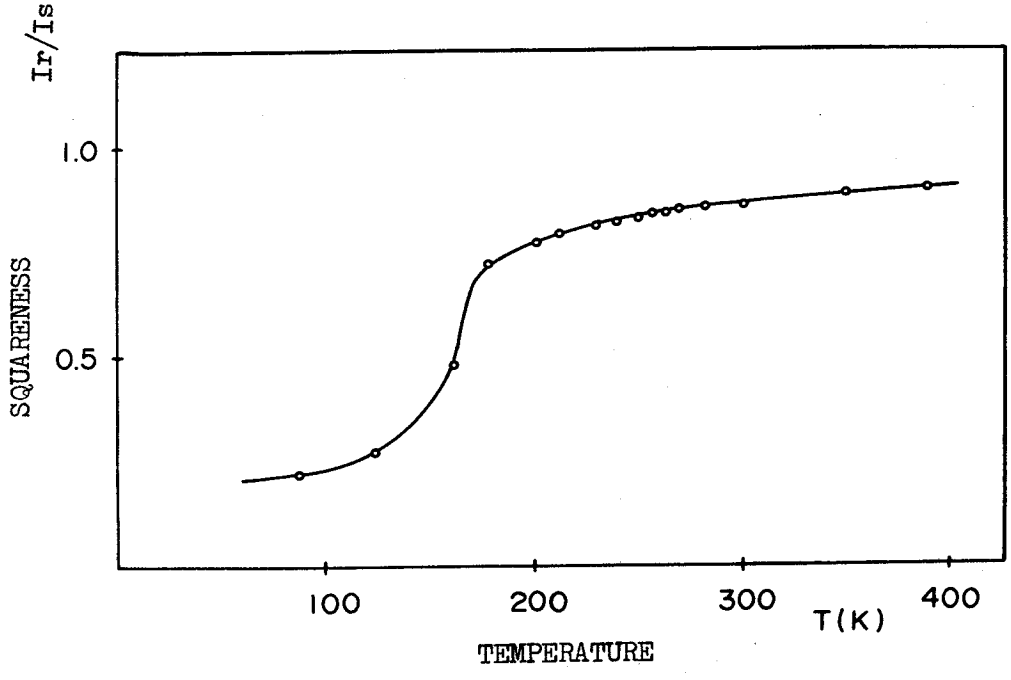

Fig. 4.9 Temperature dependence of squareness Ir/Is of MnBi particles.

domain to multi-domain. The temperature variation of remanence was measured in the temperature range from 300 to 85 K in order to observe the critical temperature at which MnBi particles cease to keep the single-domain structure.[68] The critical temperature and coercivity of MnBi particles were compared with those of sintered one.

Fig. 4.10 shows the electron micrograph of the MnBi particles used in this experiment. The particles consist of platelet-shaped crystals with diameter in the range from 0.1 to 0.25 μm and with the diameter to thickness ratio of about 10 to 1. Measurements of the coercivity and remanence were made on the sintered block and the non-oriented compact of particles pressed up to the density of approximately 5 g/cm^3, using a vibrating sample magnetometer with maximum applied field of 16000 Oe.

The coercivity of the sintered block and the particles at 85 K and 300 K is given in Table 4.1. The effect of size reduction appears obviously in the coercivity at 300 K. The high coercivity of the particles at 300 K reflects the strong crystalline anisotropy at that temperature. The small difference of coercivity at 85 K between the sintered block and the particles demonstrates that the crystalline anisotropy of MnBi becomes nearly zero at that temperature.

The temperature variation of remanence of the sintered block and the particles is shown in Fig. 4.11. The measurement was carried out by the following method. A sample was magnetized by magnetic field of 16000 Oe at 85 K, and after reaching the equilibrium state temperature was increased up to 300 K under the same magnetic field. This magnetized sample was, then, cooled down gradually from 300 K

to 85 K without the magnetic field, and warmed up again to 300 K. For sintered block, the remanence monotonously decreased with decreasing temperature. This temperature variation means that the sintered block consists almost of the multi-domain crystals in the whole range of temperature. For the particles, on the other hand, the remanence slightly increased down to about 230 K and then decreased rapidly. This temperature variation suggests that, down to about 230 K, these particles take nearly the single-domain structure. The slight increase of remanence is explained by the increase of the saturation magnetization. Since the crystalline anisotropy decreases with decreasing temperature, below about 230 K, a process of splitting into finer domains may start in the single-domain particles. Although the crystalline anisotropy becomes nearly zero at 85 K, the remanence does not become zero at that temperature. This is probably responsible for some amount of defects in the particles caused by grinding.[69] The coercivity of 11000 Oe observed at 300 K for non-oriented particles is lower than the value 14000 Oe calculated from $Hc=0.48(2K/Is - 4\pi Is)$ by the use of the values reported by Guillaud[24] and Heikes[66] for K and Is. Furthermore, in the process of cooling from 300 K to 85 K and then warming again to 300 K, the remanence of the particles exhibits a thermal hysteresis. By assuming that the critical particles diameter varies with $K^{1/2}/Is^2$, and 0.25 μm which is the largest particle diameter determined from the electron micrograph, is the critical diameter of the platelet-shaped particle at 230 K, the critical diameter at 300 K is calculated to be 0.33 μm. This value

agrees with the critical diameter of 0.5 μm which is predicted for spherical MnBi particles.

4.2.3. Relation between Anisotropy Field and Coercivity

The coercivity Hc, anisotropy constant K_1, and anisotropy field H_A were determined for the aligned MnBi particles at the temperature range where the magnetic easy axis was nearly parallel to the c-axis.[70] MnBi particles were hexagonal platelets of single crystal with a diameter from 0.1 μm to 0.3 μm. For the magnetic measurement, MnBi particles were aligned in a polymer binder along the direction of the c-axis. The packing density was about 10 volume percent.

Fig. 4.12 shows the magnetization curves of aligned MnBi particles measured parallel and perpendicular to the c-axis at room temperature. Coercivity Hc was determined from the demagnetization curve parallel to the c-axis at various temperatures. The magnetization curve perpendicular to the c-axis was measured at various temperatures in order to determine the anisotropy constant K_1.

As discussed by Sucksmith and Thompson[71], when the magnetizing field is perpendicular to the c-axis, the magnetization I measured in the direction of the magnetizing field is given by

$$Is \cdot H = 2K_1(I/Is) + 4K_2(I/Is)^3. \qquad -(1)$$

Here K_1 and K_2 are the anisotropy constant, Is is the saturation magnetization, and H is the magnetizing field perpendicular to the c-axis. Equation(1) can be rearranged in the form

$$H/I = 2K_1/Is^2 + 4K_2 \cdot I^2/Is^4. \qquad -(2)$$

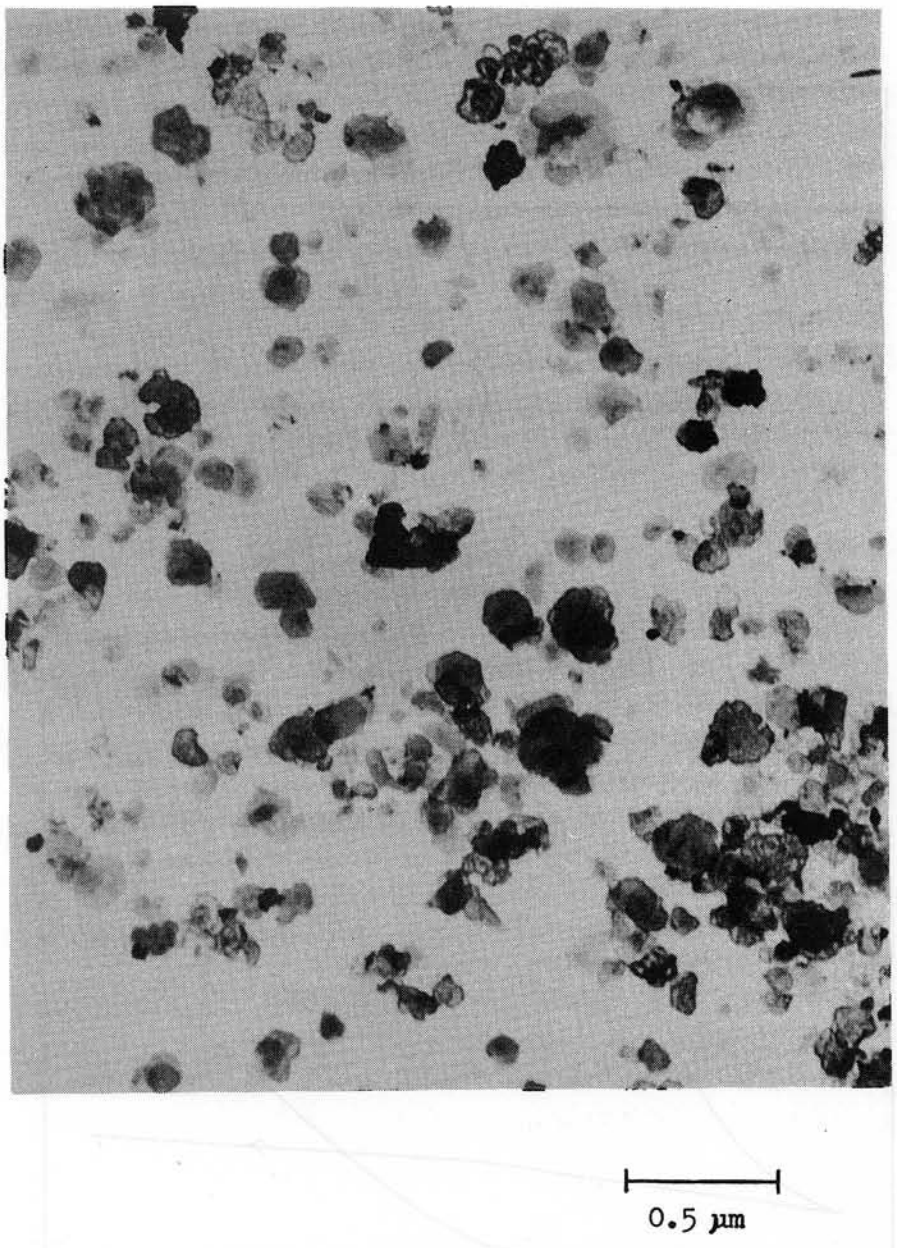

Fig. 4.10 Electron micrograph of MnBi particles.

Table 4.1 Coercivity of sintered MnBi and ball-milled MnBi particles at 85 K and 300 K.

	Hc(Oe) 85K	Hc(Oe) 300K
SINTERED	70	570
PARTICLES	320	11000

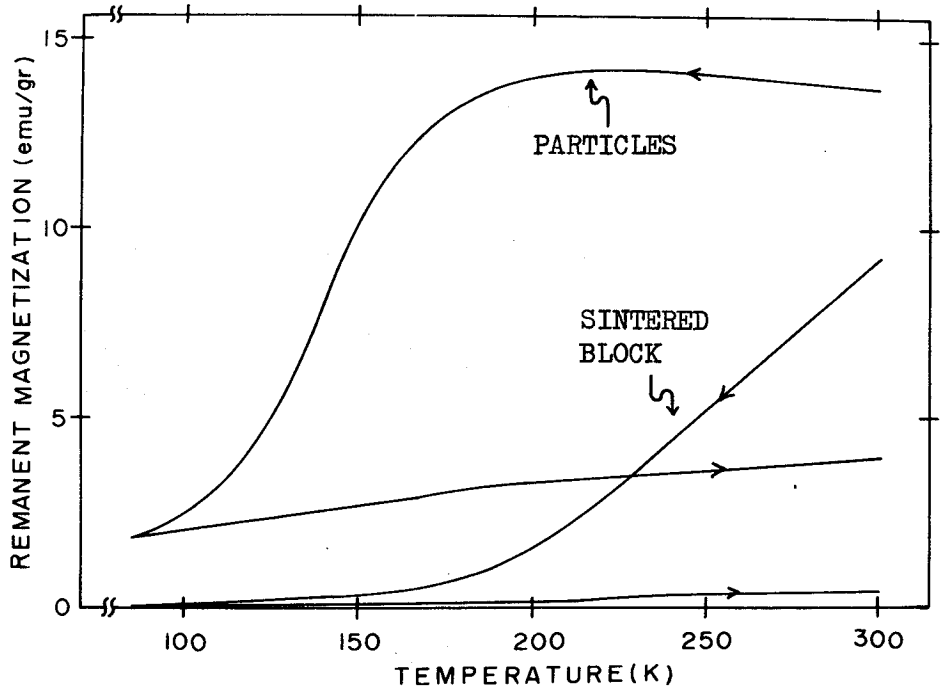

Fig. 4.11 Temperature variation of remanence for sintered MnBi and ball-milled MnBi particles.

The anisotropy constant K_1 can be calculated from the intercept $2K_1/Is^2$ by plotting a graph of Is^2 and H/I. Fig. 4.13 shows the graph of Is^2 against H/I.

The value of anisotropy energy corrected by the shape anisotropy energy at room temperature, $K_1 + 2\pi Is^2$, was 15.1×10^6 erg/cm^3, which was fairly larger than the value (8.9×10^6 erg/cm^3) reported by Guillaud.[24] In the present calculation, the Is value reported by Heikes[66] was used. For an assembly of particles, the value of shape anisotropy energy is expected to be smaller than $2\pi Is^2$ which is the value in case of an isolated particle.

Using the above mentioned data, the anisotropy field is given by $H_A = 2K_1/Is$. Fig. 4.14 shows the relation between H_A and Hc. The linear relation between H_A and Hc indicates that the magnetization reversal is nearly caused by rotating of magnetic moment itself. Below about 200 K, the deviation from the linear relation is considered to be due to the declination of the magnetic easy axis from the c-axis.

4.2.4. Stability of Remanence Observed at Low Temperature

MnBi particles are expected to be used as a stable magnetic recording material by its anomalous temperature dependence of the anisotropy energy. Informations which are recorded at such low temperature as the coercivity is small compared with that at room temperature, will be stable at room temperature due to the high coercivity. Therefore, the stability of remanence of MnBi particles which was magnetized at low temperature region such as 84 K was

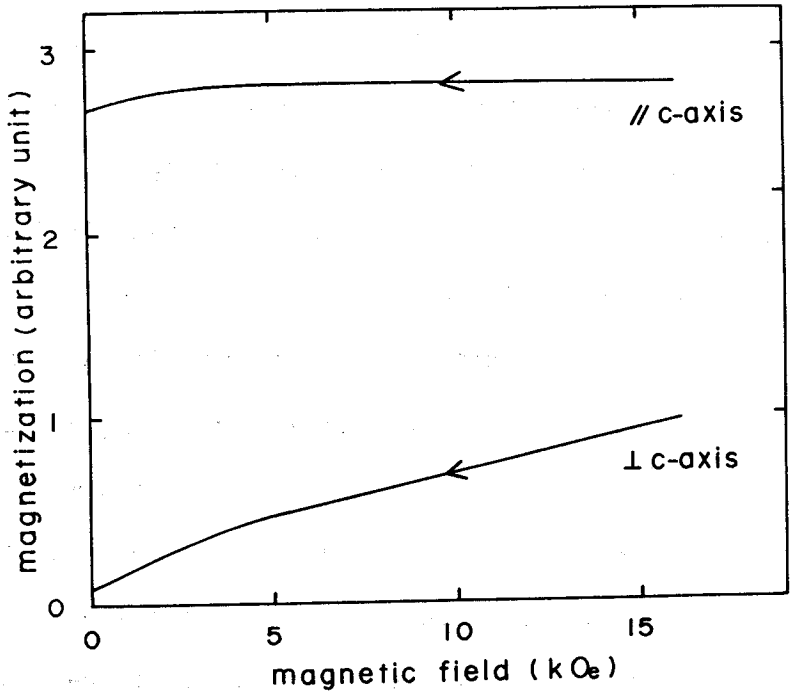

Fig. 4.12 Magnetization curves of aligned MnBi particles measured parallel and perpendicular to the c-axis at room temperature.

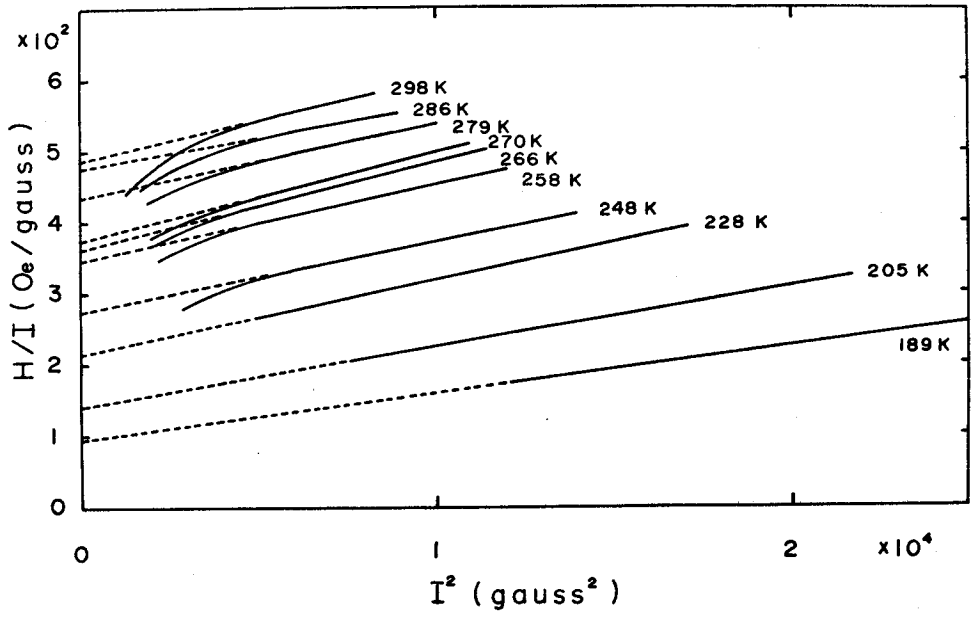

Fig. 4.13 Variation of I^2 against H/I.

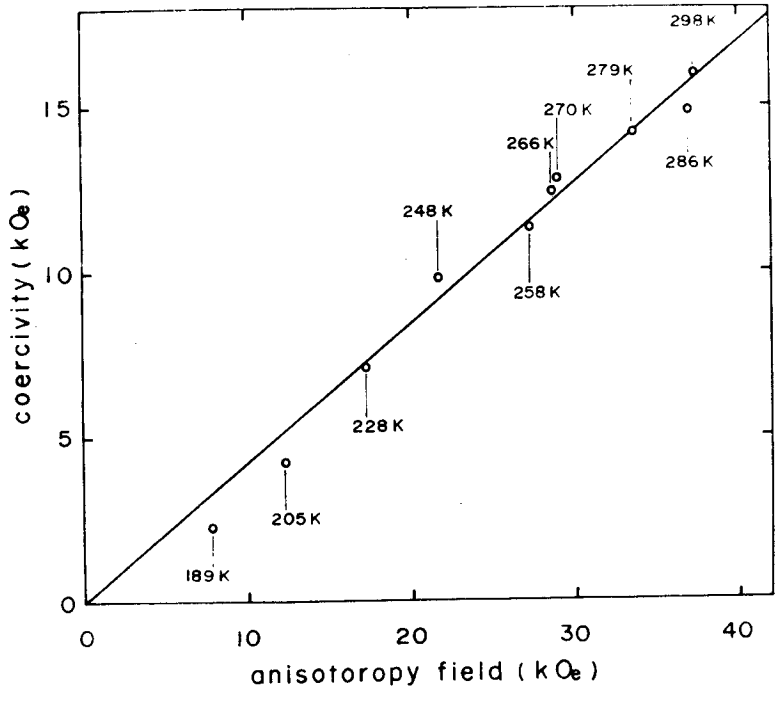

Fig. 4.14 Relation between anisotropy field H_A and coercivity Hc.

examined at room temperature.[71]

MnBi particles used in this experiment are shown in Fig. 4.15. The remanence curve on the oriented particles in polymer binder was measured by the following method. MnBi particles were cooled from room temperature to liquid nitrogen temperature under a magnetic field of various strengths. Then, the MnBi particles were warmed from liquid nitrogen temperature to room temperature under the same magnetic field. The obtained remanence is plotted as a function of the magnetic field in Fig. 4.16. The remanence nearly reaches the saturation by applying 3000 Oe. Fig. 4.17 shows the demagnetization curve of MnBi particles starting from the remanence value shown in Fig. 4.16 which was magnetized by the magnetic field of 3000 Oe and 5000 Oe. The coercivity after magnetizing by the magnetic field of 3000 Oe and 5000 Oe is 14000 Oe and 15000 Oe. Thus, MnBi particles show quite stable character.

The preferred direction of MnBi is c-axis at room temperature. On the other hand, at liquid nitrogen temperature, the basal plane is a preferred direction.[67] Therefore, when MnBi particles were warmed from liquid nitrogen to room temperature under the magnetic field, each particle would align to the same direction of the magnetic field which was applied. As shown in Fig. 4.16, MnBi particles were easily magnetized to the saturation value at about 3000 Oe. This state keeps its saturation value stably even under the reverse magnetic field at room temperature. Therefore, it is expected that informations can be recorded by comparably weak magnetic field and are kept a stable character at room

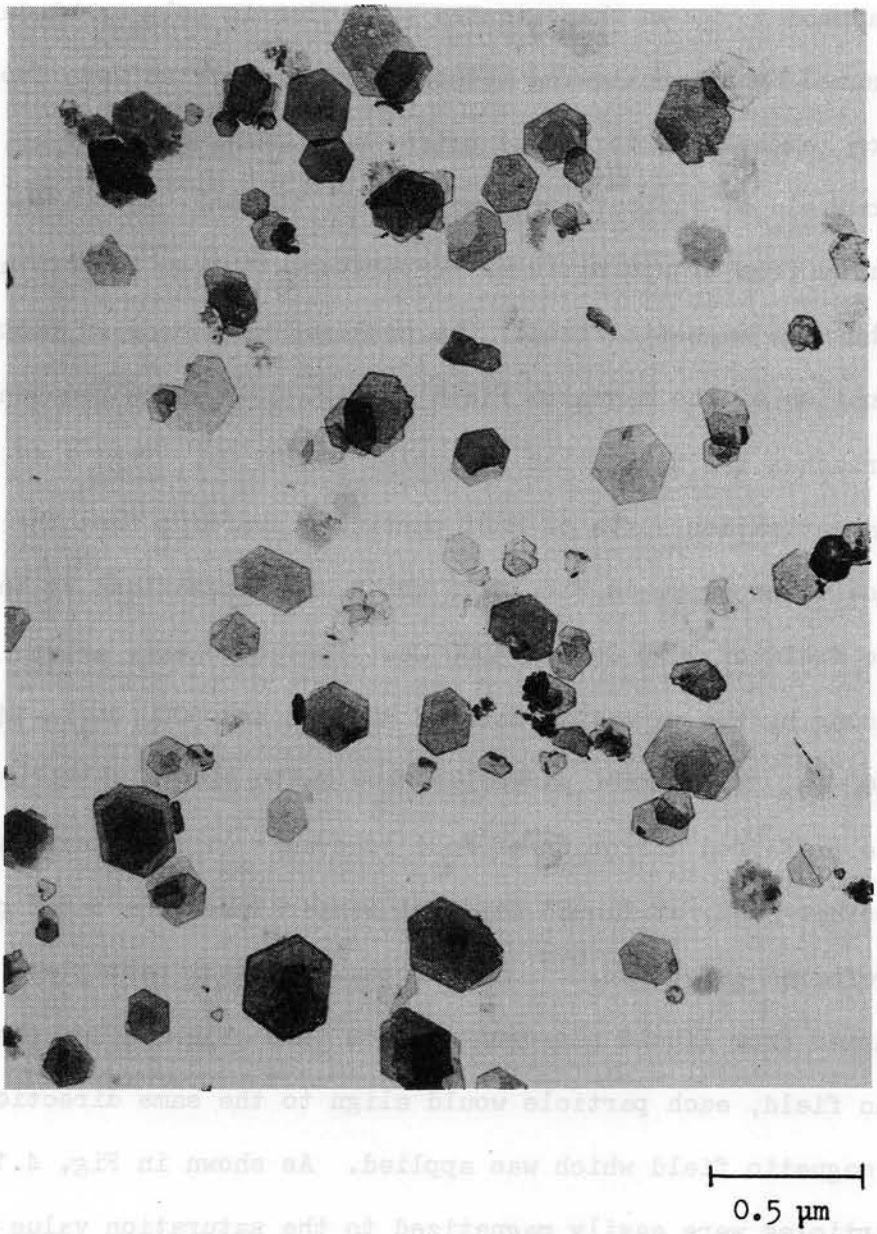

Fig. 4.15 Electron micrograph of MnBi particles.

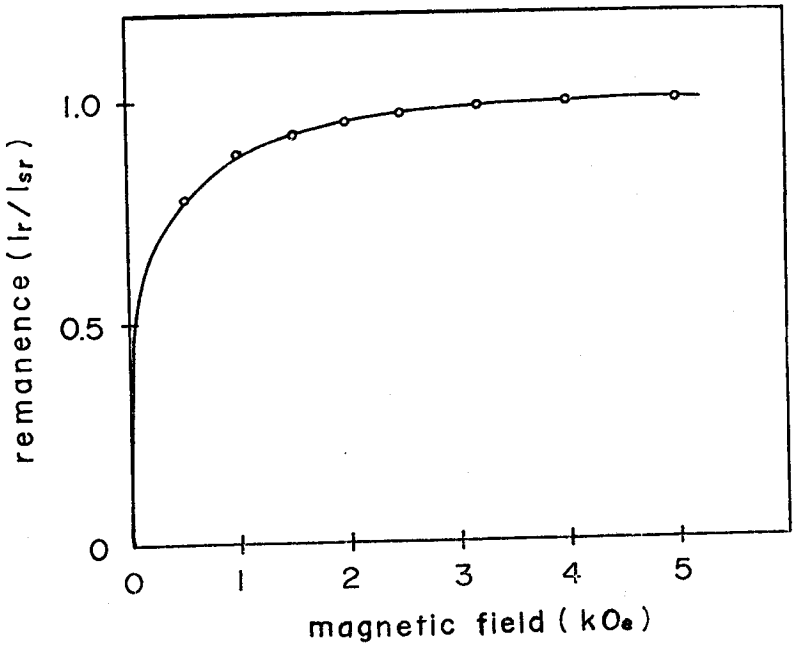

Fig. 4.16 Remanence curve of MnBi particles. Remanence was obtained by warming from liquid nitrogen temperature to room temperature under the several magnetic fields.

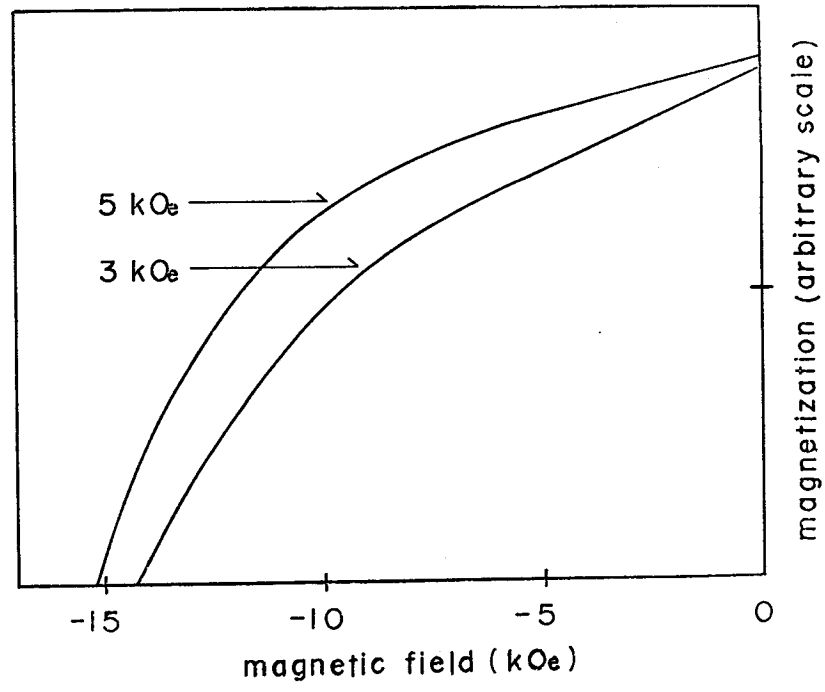

Fig. 4.17 Demagnetization curve of MnBi particles magnetized by the magnetic field of 3000 Oe and 5000 Oe starting from the remanence curve of Fig. 4.16.

temperature.

4.2.5. Stability of Remanence Observed at Room Temperature

MnBi particles are difficult to be demagnetized at room temperature due to its high coercivity. However, by utilizing the anomalous temperature dependence of coercivity, the demagnetized state could be obtained at room temperature. The remanence was measured at room temperature on the sample demagnetized by the following two methods.[73)]

Demagnetization at 84 K

The sample was first cooled from room temperature to liquid nitrogen temperature while applying the ac magnetic field of the frequency of 60 Hz and of the strength of 3000 Oe. Then, the amplitude of the ac magnetic field was reduced, and the sample was returned to room temperature. By this method, completely demagnetized state was obtained. The remanence was obtained by applying a magnetic field Hm to the demagnetized state. The result is shown with a solid curve in Fig. 4.18. The sample was magnetized easily; for instance, the magnetic field strength Hm required to obtain 50 % remanence of saturation remanence was 800 Oe. In Fig. 4.18, the saturation remanence was obtained by the following method. The sample was warmed up to room temperature from liquid nitrogen temperature while applying the magnetic field of 16000 Oe, and then the magnetic field was removed. The remanence curve suggests that the demagnetized sample is in a multi-domain state. However,

the size of MnBi particles used in this experiment is considered to be close to the critical size for single-domain behavior. When the sample is demagnetized by the method mentioned above, "nuclei", from which the magnetization reversal occurs, may exist in particles.

ac magnetic field treatment at room temperature

The ac magnetic field of 6500 Oe was further applied at room temperature to the demagnetized sample by the method mentioned above. The remanence measured after the ac magnetic field treatment is shown with a dotted curve in Fig. 4.18. The sample treated in this way was in the state to be difficult to be magnetized; for instance, by applying Hm of 5000 Oe, only 8 % remanence of saturation remanence was obtained. This result is explained in the following manner. The magnetization of each oriented particle in the sample is fixed in the positive or negative direction along the c-axis in the process of reducing ac magnetic field gradually from 6500 Oe to zero. For the particles which approach saturation, a strong magnetic field is required to reverse the direction of magnetization in particles. The "nuclei", which exist in the demagnetized state obtained in cooling, can be considered to disappear by applying higher magnetic field. The whole magnetization of the sample becomes zero by cancelling the magnetization of each particle.

In order to examine the disappearance of the "nuclei" in particles, the magnetic-field-strength dependence of coercivity was measured. Fig. 4.19 shows the properties of the samples of

second-quadrant region with various remanence values which are plotted in the solid curve in Fig. 4.19. The coercivity after applying Hm of 3000, 5000, 10000, and 16000 Oe is about 5000, 8000, 12000, and 16000 Oe, respectively. On the other hand, the remanence obtained by applying Hm of 3000, 5000, 10000, and 16000 Oe is about 90, 93, 96, and 98% of saturation remanence, respectively. Although the coercivity remarkably increased with increasing Hm, the remanence increased only slightly. From these results, it is concluded that the magnetization reversal in MnBi particles is caused by the "nuclei", and the "nuclei" disappear by applying strong magnetic field.

It is clear that the remanence obtained at room temperature also showed the stability not to be demagnetized easily. The device to magnetize MnBi particles at room temperature is more promising than the device to magnetize at low temperature, which is described in 4.2.4, from practical use because of the easiness of magnetization device.

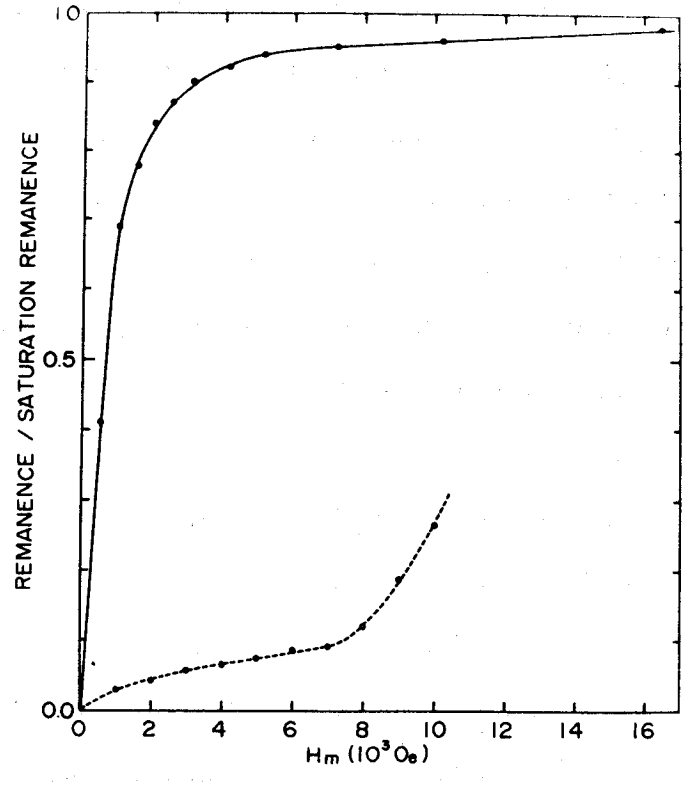

Fig. 4.18 Remanence curve of MnBi particles. Solid and dotted curve show the results of measurement after demagnetization at 84 K and ac magnetic field treatment at room temperature, respectively.

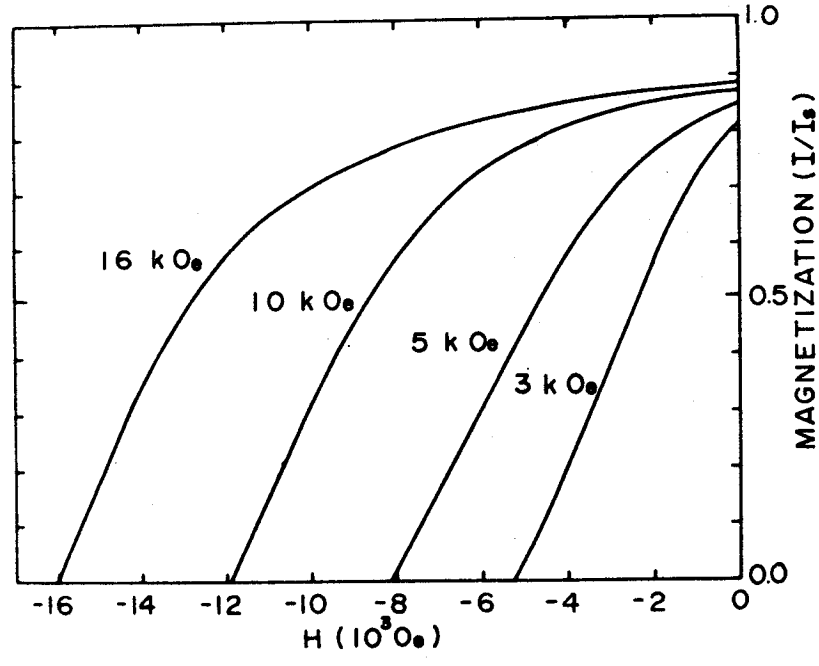

Fig. 4.19 Second-quadrant properties of MnBi particles which were magnetized by applying various strengths of magnetic field.

5. Summary

The magnetic recording material is classified into three classes such as that of γ-Fe_2O_3 particles, that of cobalt-contained iron oxides, and that of MnBi particles according to the strength of coercivity. The effect of the magnetic anisotropies influencing the coercivity of the each material was studied in detail.

5.1. γ-Fe_2O_3 Particles

Effect of crystallite size on the coercivity of γ-Fe_2O_3 particles was studied for samples prepared by dehydrating α-FeOOH in various temperatures. Following results were obtained.

1) The crystallite size of γ-Fe_2O_3 particles of the highest coercivity was about 450 Å which nearly agreed with the calculated critical size of single-domain behavior.

2) Superparamagnetic behavior was observed even in the γ-Fe_2O_3 particles having average crystallite size of 500 Å. The broad distribution of crystallite size in the particles was indicated.

3) The lowering of coercivity of γ-Fe_2O_3 particles prepared by dehydrating at 800°C was attributed to the decrease of shape anisotropy.

5.2. Cobalt-Substituted Iron Oxide Particles

A magnetic material having higher coercivity than γ-Fe_2O_3 particles is required as a better recording substance. Cobalt-substituted iron oxides were developed for this purpose. The material has the advantage that the coercivity can easily be increased by substituting some small amount of iron with cobalt ions. However, this material has an unamenable disadvantage

that the magnetic properties become unstable not only at high temperature but also during the aging. The origin of instability of coercivity was studied for the cobalt-substituted iron oxides with various content of Fe^{2+} and Co^{2+} ions. Following results were obtained.

1) For the samples containing Fe^{2+} more than 1 wt%, the coercivity remarkably increased by the annealing at 60°C. For the samples containing Fe^{2+} less than 1 wt%, the increase of coercivity by the annealing was not observed.

2) The increase of coercivity was attributed to the magnetic anisotropy induced by the migration of Co^{2+} ions to the stable sites in the direction of demagnetizing magnetic field due to shape anisotropy.

3) The existence of Fe^{2+} was considered to facilitate the migration of Co^{2+} ions.

4) The coercivity of the samples containing Fe^{2+} of 22-23 wt% linearly increased with Co^{2+} content. This meant that the effect of crystalline and induced anisotropy was additive and proportional to cobalt content in the samples containing cobalt of 0.5-2.4 wt%.

To increase the coercivity of γ-Fe_2O_3 particles, iron-cobalt ferrite was crystallized only on the surface of γ-Fe_2O_3 particles without substituting iron ion by cobalt ion. The special method of producing and magnetic properties were studied . Following results were obtained.

1) These oxides were prepared by heating γ-Fe_2O_3 particles at

90°C in alkaline solution containing Co^{2+} and Fe^{2+}.

2) The coercivity of the oxides remarkably increased with increasing Co^{2+}/Fe^{2+} ratio, and in the neighbourhood of the Co^{2+}/Fe^{2+} ratio of 0.4-0.5, reached a maximum value.

3) The variation of morphology of particles to occur in the heat-treatment was examined by the electron micrographs. It was proved that iron-cobalt ferrite crystallized only on the surface of γ-Fe_2O_3 particles.

4) When the oxides with Co^{2+}/Fe^{2+} ratio of 0.5 were immersed in hydrochloric acid, both the cobalt content and the coercivity were rapidly decreased with the dissolved weight. This result showed that the increase of coercivity was attributed to the iron-cobalt ferrite on the surface of γ-Fe_2O_3 particles.

5) The coercivity of the oxides with Co^{2+}/Fe^{2+} ratio of 0.5 linearly increased with cobalt content. The magnetic anisotropy of the iron-cobalt ferrite was expected to be nearly parallel to the direction of the shape anisotropy of γ-Fe_2O_3 particles.

6) The coercivity of the oxides was extremely stable for temperature and time compared with that of cobalt-substituted iron oxides. The stability was explained by considering that high concentration of Co^{2+} ions existed on the γ-Fe_2O_3 particles, and the migration of Co^{2+} ions was difficult.

5.3. MnBi Particles

For the material having the coercivity higher than 2000 Oe, MnBi particles are promising. MnBi particles have the possibility

to be utilized for permanent recording material. The method to prepare particles of MnBi having special magnetic properties available for the permanent recording material was studied. Following results were obtained.

1) Mn-Bi compound showed the highest saturation magnetization of 79 emu/g at 85 K in the composition of $Mn_{55}Bi_{45}$.

2) At 300 K, the coercivity of MnBi particles remarkably increased with reduction of particle size, and the highest coercivity of 16000 Oe was observed.

3) At 85 K, the coercivity was about 80-400 Oe, low compared with that of 300 K.

4) The temperature dependence of coercivity of platelet-shaped particles with average diameter of 0.5 μm was explained from the crystalline anisotropy of MnBi and the shape anisotropy of particles.

5) MnBi particles having the coercivity about 10000 Oe at room temperature could be demagnetized easily by cooling down to liquid nitrogen temperature.

6) MnBi particles demagnetized at liquid nitrogen temperature could be magnetized easily even at room temperature.

7) The coercivity at room temperature of the demagnetized particles remarkably increased with increasing the strength of applied magnetic field.

8) When ac magnetic field of 6500 Oe was applied to the demagnetized particles, the MnBi particles became extremely difficult to be magnetized at room temperature.

9) The results of 5)-8) suggested that "nuclei" from which magneti-

zation reversal occured existed in particles in the demagnetized state, and disappeared by applying a strong magnetic field.

Acknowledgements

I wish to express my sincere thanks to Late Professor N. Kawai of Osaka University for reading and criticism of the manuscript, and helpful discussions of this study, and to Professor T. Haseda of Osaka University for reading of the manuscript and discussions with great kindness. Thanks are also due to Professor A. Tasaki of Tsukuba University for valuable suggestions and continuous encouragement during the course of this study. I also thank to Dr. I. Tochikubo, the Head and Director of Technical Research Laboratory of Hitachi Maxell Co. Ltd., and Dr. F. Hayama, Manager and Director of Technical Research Laboratory of Hitachi Maxell Co. Ltd. for guidance and encouragement during the course of this study. I am also indebted to Dr. M. Amemiya and Mr K. Wakai of Technical Research Laboratory of Hitachi Maxell Co. Ltd. for kind guidance, much help, and fruitful discussions for this study.

References

1) M. Camras: U. S. Patent 2 694 656 (1954).

2) G. Bate and J. Alstad: IEEE Trans. Magnetics MAG-5 (1969) 821.

3) Y. Yada, S. Miyamoto, and H. Kawagoe: IEEE Trans. Magnetics MAG-9 (1973) 185.

4) B. Gustard and M. R. Wright: IEEE Trans. Magnetics MAG-8 (1972) 426.

5) G. Guillaud, A. Michel, J. Benard, and M. Fallot: C. R. Hebd. Sean. Acad. Sci. 219 (1944) 58.

6) F. J. P. Svoboda, A. Arthur, W. L. Cox, J. N. Ingraham, A. L. Oppegard, and M. S. Sadler: J. Appl. Phys. Suppl. 32 (1961) 373.

7) Du Pont: French Patent 1 154 191 (1958).

8) D. E. Speliotis, J. R. Morrison, and G. Bate: Proc. Int. Conf. on Magnetism, Nottingham (1964).

9) K. E. Nauman and E. D. Daniel: J. Aud. Eng. Soc. 19 (1971) 822.

10) A. A. van der Giessen: Rev. Phys. appl. 9 (1974) 869.

11) H. Takei and S. Chiba: J. Phys. Soc. Japan 21 (1966) 1255.

12) T. Namikawa and S. Tochihara: IEEE Trans. Magnetics MAG-9 (1973) 188.

13) D. S. Rodbell: J. Phys. Soc. Japan 21 (1966) 2430.

14) AMPEX: U. S. Patent 3 748 270 (1971).

15) 3M-COMPANY: U. S. Patent 3 573 980 (1971).

16) TODA-KOGYO: U. S. Patent 3 720 618 (1973).

17) SONY: Dutch Pat. Appl. 7 301 614 (1973).

18) S. Nobuoka, T. Ando, and F. Hayama: U. S. Patent 3 081 264 (1963).

19) 3M-COMPANY: German Pat. Appls. 2 326 258 (1973).

20) A. A. van der Giessen and C. J. Klomp: IEEE Trans. Magnetics MAG-5 (1969) 317.

21) K. Kusaka, N. Wada, and A. Tasaki: Japan J. appl. Phys. 8 (1969) 599.

22) M. Kawasaki and S. Higuchi: IEEE Trans. Magnetics MAG-8 (1972) 552.

23) K. Adachi: J. Phys. Soc. Japan 16 (1961) 2187.

24) C. Guillaud: J. Phys. Radium 12 (1951) 492.

25) B. W. Roberts: Phys. Rev. 104 (1956) 607.

26) M. Kishimoto and K. Wakai: Japan. J. appl. Phys. 16 (1977) 2059.

27) L. Alexander and H. P. Klug: J. Appl. Phys. 21 (1950) 137.

28) F. W. Jones: Proc. Roy. Soc. A166 (1938) 16.

29) A. H. Morrish and S. P. Yu: J. Appl. Phys. 26 (1955) 1049.

30) A. E. Berkowitz and W. J. Schuele: J. Appl. Phys. 39 (1968) 1261.

31) E. P. Wohlfarth: Proc. Roy. Soc. (London), A 232, (1955) 208.

32) I. S. Jacobs and C. P. Bean: Phys. Rev. 100 (1955) 1060.

33) I. S. Jacobs and F. E. Luborsky: J. Appl. Phys. 28 (1957) 467.

34) A. Yanase: J. Phys. Soc. Japan 17 B-1 (1962) 1005.

35) R. M. Bozorth, E. F. Tilden, and A. J. Williams: Phys. Rev. 99 (1955) 1788.

36) R. F. Penoyer and L. R. Bickford: Phys. Rev. 108 (1957) 271.

37) S. Iida and T. Inoue: J. Phys. Soc. Japan 17 B-1 (1962) 281.

38) M. Kishimoto, J. Hirata, and F. Hayama: Journal of the Japan Society of Powder and Powder Metallurgy 26 (1979) 49 (in Japanese).

39) M. Kishimoto and J. Hirata: Papers of Technical Group on Magnetic Recording, I. E. C. E. (Japan) MR 77-27 (1978) 1 (in Japanese).

40) M. Kishimoto: IEEE Trans. Magnetics MAG-15 (1979) 906.

41) F. Hayama, I. Tochikubo, and Y. Soezima: OYO BUTURI 35 (1966) 797 (in Japanese).

42) H. J. Williams, R. D. Heidenreich, and E. N. Nesbitt: J. Appl. Phys. 27 (1956) 85.

43) L. Neel: Rev. mod. Phys. 25 (1953) 293.

44) G. Bate: AIP Conference Proceedings Vol 1, No 5 (1971) 766.

45) E. Koster: J. Appl. Phys. 41 (1970) 3332.

46) M. Kishimoto, T. Sueyoshi, J. Hirata, M. Amemiya, and F. Hayama: J. Appl. Phys. 50 (1979) 450. M. Amemiya, M. Kishimoto, and F. Hayama: to be published in IEEE Trans. Mangnetics MAG-16 (1980).

47) M. Kishimoto, T. Sueyoshi, S. Kitaoka, K. Wakai, and M. Amemiya: Journal of the Japan Society of Powder and Powder Metallurgy 26 (1979) 31 (in Japanese). M. Kishimoto, K. Sumiya, and F. Hayama: to be published in Journal of the Japan Society of Powder and Powder Metallurgy 27 (1980) No 1.

48) L. R. Bickford, J. M. Brownlow, and R. F. Penoyer: Proc. Inst. Elec. Eng. 104B (1957) 238.

49) Y. Tokuoka, S. Umeki, and Y. Imaoka: J. Physique 38 C1 (1977) 337.

50) C. Guillaud: J. Phys. Radium 12 (1951) 143.

51) H. J. Williams, R. C. Sherwood, and O. L. Boothby: J. Appl. Phys. 28 (1957) 445.

52) W. M. Yim and E. J. Stofko: J. Appl. Phys. 38 (1967) 5211.

53) D. Chen, G. N. Otto, and F. M. Schmit: IEEE Trans. Magnetics MAG-9 (1973) 66.

54) S. Honda and T. Kusuda: J. Appl. Phys. 45 (1974) 2689.

55) B. Tsujikawa, S. Yoshii, and K. Nishiguchi: IEEE Trans. Magnetics MAG-8 (1972) 603.

56) E. Adams, W. M. Hubbard, and A. M. Syeles: J. Appl. Phys. 23 (1952) 1207.

57) E. Adams: Rev. mod. Phys. 25 (1953) 306.

58) E. P. Wolfath: Advanc. Phys. 8 (1959) 87.

59) P. A. Albert and W. J. Carr: J. Appl. Phys. 32 (1961) 201S.

60) T. Hihara and Y. Koi: J. Phys. Soc. Japan 29 (1970) 343.

61) E. V. Shtoltz, J. S. Shur, and G. S. Kandurova: Izv. Akad. Nauk. SSR 22 (1958) 1269.

62) Seybolt, Hansen, Roberts, and Yurisin: J. Metals 8 (1956) 606.

63) N. Makino and M. Suzuki: Journal of the Japan Institute of Metals 24 (1960) 24 (in Japanese).

64) M. Takahashi: Trans. JIM 12 (1971) 307.

65) M. Kishimoto and K. Wakai: Japan J. appl. Phys. 16 (1977) 459.

66) R. R. Heikes: Phys. Rev. 99 (1955) 446.

67) M. Kishimoto and K. Wakai: Japan J. appl. Phys. 14 (1975) 893.

68) M. Kishimoto and K. Wakai: Japan J. appl. Phys. 15 (1976) 1843.

69) J. J. Becker: IEEE Trans. Magnetics MAG-5 (1969) 211.

70) M. Kishimoto and K. Wakai: Japan J. appl. Phys. 15 (1976) 549.

71) W. Sucksmith and J. E. Thompson: Proc. Roy. Soc. (London) 225 (1954) 362.

72) M. Kishimoto and K. Wakai: Japan J. appl. Phys. 14 (1975) 1257.

73) M. Kishimoto and K. Wakai: J. Appl. Phys. 48 (1977) 4640.